Keep the bees off the trees: the vulnerability of species in the periphery of mutualistic networks to shock perturbations

To cite this article: Lukas Halekotte *et al* 2025 *J. Phys. Complex.* **6** 035002

IOP Publishing J. Phys. Complex. 6 (2025) 035002 https://doi.org/10.1088/2632-072X/ade927

Journal of Physics: Complexity

OPEN ACCESS

RECEIVED
18 December 2024

REVISED
20 May 2025

ACCEPTED FOR PUBLICATION
27 June 2025

PUBLISHED
8 July 2025

PAPER

Keep the bees off the trees: the vulnerability of species in the periphery of mutualistic networks to shock perturbations

Lukas Halekotte[1,2,*], **Anna Vanselow**[1] and **Ulrike Feudel**[1]

[1] Institute for Chemistry and Biology of the Marine Environment, Carl von Ossietzky University Oldenburg, Oldenburg, Germany
[2] German Aerospace Center (DLR), Institute for the Protection of Terrestrial Infrastructures, Sankt Augustin, Germany
[*] Author to whom any correspondence should be addressed.

E-mail: lukas.halekotte@uol.de

Keywords: multistability, shock-tipping, complex networks, mutualistic networks, plant-pollinator networks, centrality indices, core-periphery structure

Abstract

We study the phenomenon of multistability in mutualistic networks of plants and pollinators, where one desired state in which all species coexist competes with multiple states in which some species are gone extinct. In this setting, we examine the relation between the endangerment of pollinator species and their position within the mutualistic network. To this end, we compare endangerment rankings which are derived from the species' probabilities of going extinct due to random shock perturbations with rankings obtained from different network theoretic centrality metrics. We find that a pollinator's endangerment is strongly linked to its degree of mutualistic specialization and its position within the core-periphery structure of its mutualistic network, with the most endangered species being specialists in the outer periphery. Since particularly well established instances of such peripheral areas are tree-shaped structures which stem from links between nodes/species in the outermost shell of the network, we summarized our findings in the admittedly ambiguous slogan *keep the bees off the trees*. Finally, we extend the mutualistic system to a multilayer network, where a species' position in the mutualistic network layer determines its position in a competitive network layer. We find that this multilayer setup, that allows peripheral species to avoid competition, can lead to very similar endangerment rankings as the standard setup under harsh environmental conditions, but to very different rankings under favorable conditions.

1. Introduction

Mutualism is defined as an interaction between two species from which both benefit [1, 2]. A popular example of a mutualistic interaction is a bee which visits flowers to collect pollen or drink nectar and thereby facilitates the pollination of the visited plants, i.e. the pollinator receives food (+), the plant the service of pollination (+). If one considers not only the mutualistic interaction between two species but between all plant and pollinator species within an ecosystem, one ends up with a complex mutualistic network in which each node represents either a plant or a pollinator species and each link denotes that the pollinator at the one end of the link has been observed to visit the plant species at the other end (figure 1(a)).

The network of interactions between plants and pollinators yields non-random complex patterns [3, 4] whose specifics affect the dynamics and the stability of the corresponding ecosystems [5–10]. Importantly, the individual contribution to the overall system functioning and robustness varies widely among species—e.g. the loss of particular keystone species can trigger extinction cascades [5, 11–13]. However, just like the importance, also the vulnerability of species is distributed unevenly—which has led to non-random losses of species in the past [14, 15]. Differences in the importance and vulnerability of species can be associated with differences in topological properties of the corresponding nodes [13, 16]. For instance, the endangerment of species with few connections (specialists) has been highlighted multiple times [15, 17] and the importance of specific species with many connections (generalists) is amplified due to the disassortative mixing within plant–pollinator networks, especially due to the tendency of specialists to interact with generalists [4, 18].

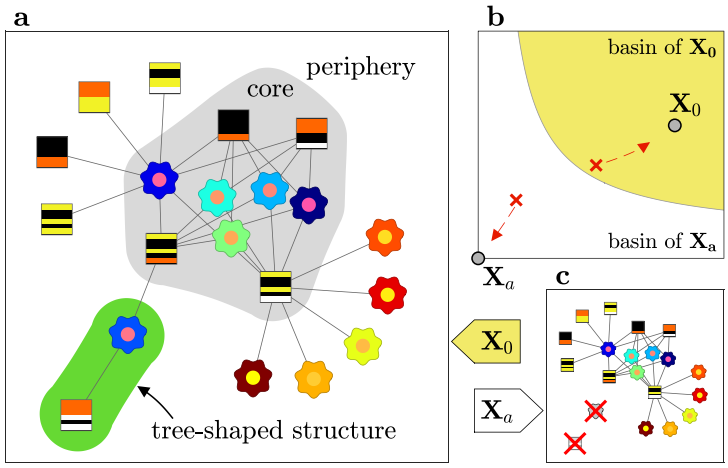

Figure 1. Core-periphery structure and multistability in a plant–pollinator network. (a) Exemplary plant–pollinator network exhibiting a core-periphery structure with a single tree-shaped part (highlighted in green). The network is bipartite with links existing only between plant (flowers) and pollinator (squares) species. (b) Exemplary phase space with two basins of attraction, one corresponding to the desired state $\mathbf{X_0}$ (yellow) in which all species coexist and one to an alternative undesired state $\mathbf{X_a}$ (white) in which some species are extinct. The two initial conditions (red crosses) depict a non-fatal and a fatal perturbation leading to the two opposing attractive states. (c) Network depiction of an alternative state in which two species are lost.

The tendency for asymmetric interactions paired with a heterogeneous degree distribution (many specialists, fewer generalists) results in a global network structure which can be divided into a rather densely connected core and a periphery of specialists which are mostly linked to generalists in the core [4, 19–21] (figure 1(a)). A simple approach to capture this core-periphery division is the k-shell decomposition [22] which assigns nodes to different shells based on the following procedure: All nodes of degree $k = k_s = 1$ are recursively removed and assigned to the 1-shell until no such nodes remain. To create the higher order shells, k_s is then stepwise increased and the procedure—recursively remove nodes with degree $k \leqslant k_s$ and assign them to the k_s-shell—is repeated until each node has been assigned to a shell. Accordingly, nodes in the inner core receive a high shell index, while the most peripheral species are in the 1-shell (e.g. all specialists and the two nodes in the tree-shaped structure in figure 1(a)). The significance of the core-periphery distribution of plant–pollinator networks was highlighted by Morone *et al* [23]. Using the k-shell decomposition, they showcased that the gradual collapse of a mutualistic network follows the core-periphery distribution, with nodes/species in the outermost periphery being lost first, while the loss of nodes in the innermost core signals the advent of a complete system collapse.

The work by Morone *et al* [23] is part of a series of theoretical works examining the robustness of mutualistic networks in the light of changing environmental conditions [24–31]. Studying corresponding scenarios is valuable for understanding, predicting and potentially countering the systemic response of mutualistic networks to an ongoing environmental deterioration [32]. In this context, it is important to note that mutualistic networks are nonlinear dynamical systems which, due to the positive interactions between species, inevitably involve positive feedbacks [25, 33, 34]. Positive feedbacks can reinforce the impact of an initial change and thus allow for an abrupt response to the gradual environmental change. The most severe instance is a so-called tipping point [35], which, if approached due to a parameter surpassing a critical threshold, leads to a partial or even complete system collapse. Important insights provided by tipping-related studies are that specialists or generally species in the periphery of mutualistic networks are the ones being affected first as conditions are becoming critical [23, 25, 26], while central species and species in the core are most essential for the integrity of the whole system [23, 27, 30].

In a scenario of smoothly and slowly changing conditions, a system can only tip or collapse if a bifurcation is approached at which the present desired system state is replaced by an alternative undesired one. However, not only the system response but also disturbances can be large and occur abruptly. Prominent examples of such shock perturbations are extreme events like floods, dry periods or wildfires [36]—all of which represent extreme stressors for populations [37–41]. In mutualistic networks, large shock perturbations are particularly significant as the characteristic positive feedbacks are likely to induce multistability [33]—especially in systems with obligatory mutualism [42]. Multistability describes the phenomenon that the phase space is populated by multiple coexisting basins of attraction (figure 1(b)), where each basin comprises all initial conditions which lead to the same attractor or stable long-term behavior. In plant–pollinator networks, one of these attractors can be considered the desired state in which

all species coexist ($\mathbf{X_0}$ in figure 1), while all others are considered undesired states in which some species are lost or extinct ($\mathbf{X_a}$ in figure 1). Accordingly, a shock perturbation can be fatal if it pushes the system into the basin of any undesired state. As such shock-induced transitions can occur long before a bifurcation point, no prior trend precedes the event, no early warning signals can be detected [26, 43] and its consequences are hard to predict [28].

In an earlier study, Halekotte and Feudel [44] determined the most efficient way to trigger such a shock-induced transition from the basin of the desired to the basin of an undesired state for different plant–pollinator networks. They found that motifs which turned out to be particularly vulnerable involved links between multiple peripheral nodes. The most outstanding instances of such peripheral motifs are tree-shaped or tree-like structures (figure 1(a)). A tree-shaped structure [45] can be defined as a connected subgraph which is located entirely in the 1-shell and thus, if cut from the rest of the network, fulfills the definition of a tree (it contains no circles), while a tree-like structure is one which resembles a tree-shaped structure. Accordingly, the findings by Halekotte and Feudel [44] highlight the particular significance of peripheral, tree-like structures (*the trees*) for the vulnerability of mutualistic species to shock perturbations.

However, the consideration of single specific perturbations only provides insights concerning the endangerment of a small set of particularly vulnerable species. In this work, we provide information on the endangerment of all species—also including less endangered species. To this end, we consider plant–pollinator networks as nonlinear dynamical systems (section 2.1) exhibiting multistability—with one desired and multiple undesired states. As in [44], we assume that these systems are subject to large abrupt disturbances which directly affect their state variables. More specifically, we examine how likely a species is to go extinct due to a single large shock perturbation (section 2.2). However, in contrast to [44], we consider random instead of specific perturbations. The use of a set of random perturbations allows us to derive an endangerment ranking—ranking all pollinator species from most to least prone to getting extinct. In order to capture the relation between a species' endangerment and its position in the network, we compare the endangerment ranking to rankings which are derived from structural properties of the underlying network topology—i.e. rankings which are based on centrality metrics (section 2.3). In this context, we aim for ranking algorithms which are ecologically meaningful as well as easy to interpret—in particular, we apply centrality metrics which take into account the degree of specialization, the core-periphery structure of plant–pollinator networks and/or the mutual enforcement between mutualistic partners.

In the remainder of this work, we proceed as follows: We first illustrate the general idea of our work and introduce the necessary tools for our analysis, which include the dynamical model of mutualism, the procedure for creating the endangerment rankings and the selection of applied topological ranking algorithms (section 2). By applying these tools to different empirical plant–pollinator networks, we then test which centrality metric best reflects the distribution of species endangerment within mutualistic networks (section 3). We then proceed to investigate how changing environmental conditions can affect the distribution of species endangerment, first in our standard system setup (section 4) and then in an alternative setup which involves a non-trivial topology for the competition between species (section 5). In this context, we also use a composite of different centrality metrics to illustrate how certain topological traits of network nodes contribute to the endangerment of the corresponding species. Finally, we conclude with a discussion of our findings (section 6).

2. Methods: endangerment and peripheriness rankings

In short, the core idea of this work is to rank the pollinator species within plant–pollinator systems according to their probability of getting extinct (endangerment ranking, figure 2(a)) and according to their position within the corresponding network (peripheriness ranking, figure 2(b)), and then compare those rankings. It should be noted that, in line with this core idea, the results in figure 4 (section 3) represent the centerpiece of this work. In the following, we present the tools required to obtain the different rankings, (1) for the endangerment ranking: the dynamical model of the plant–pollinator system (section 2.1) and the applied perturbation/simulation scheme (section 2.2), and, (2) for the peripheriness ranking: an overview over the selected ranking algorithms (section 2.3).

2.1. Model of plant–pollinator networks

We consider a simple model of a mutualistic network [6, 25] in which the dynamics of each species, plant P or animal pollinator A, are captured in a differential equation including a term for the intrinsic dynamics f_i, the interspecific competition g_i and the mutualistic interaction m_i. The latter is combined with an Allee effect q_i. For the abundance of an exemplary plant species P_i, the dynamics read

$$\frac{\mathrm{d}P_i}{\mathrm{d}t} = \left[f_i(P_i) - g_i(\mathbf{P}) + q_i(P_i)\, m_i(\mathbf{A})\right] P_i \ , \tag{1}$$

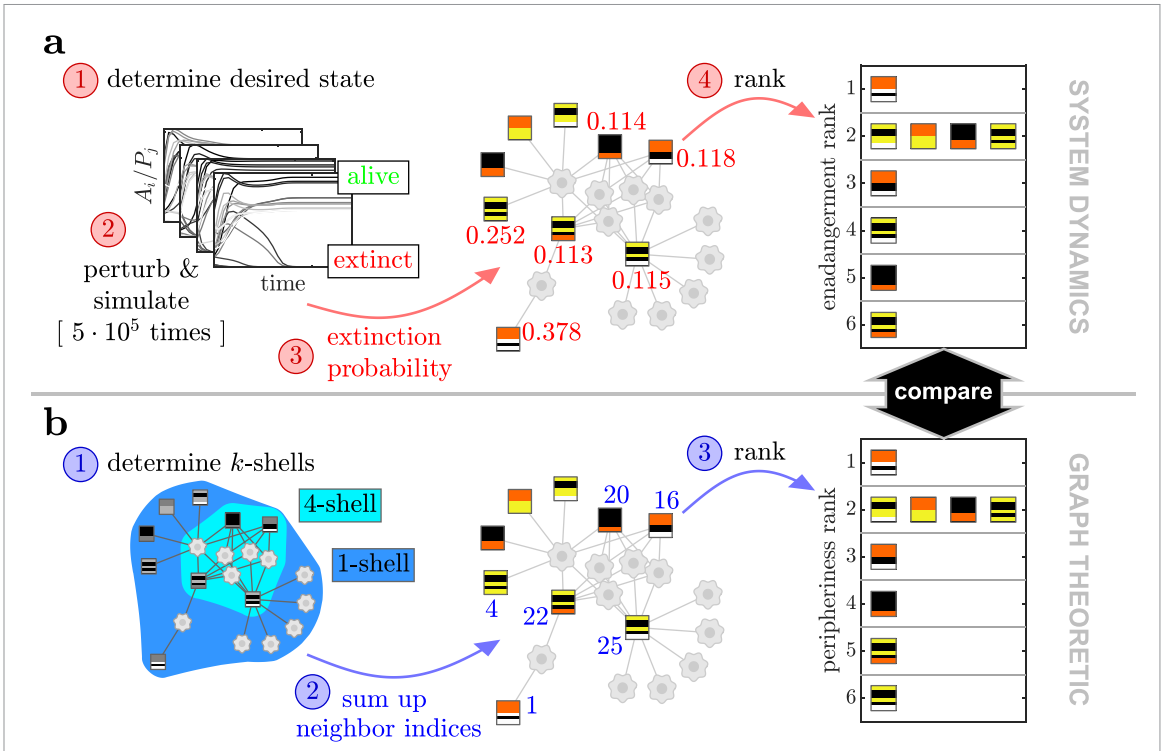

Figure 2. Creation of endangerment and peripheriness rankings. (a) Upper half of the figure illustrates the creation of the endangerment ranking (red numbering): (1) Set up dynamical system and determine its desired state in which all species coexist; (2) perturb desired state and simulate system until final stable state is reached, repeat this N_Δ times; (3) extinction probability for each species is obtained by counting the number of final states in which the species is extinct and dividing it by the total number of simulations N_Δ; (4) rank species in descending order of extinction probability. (b) Lower half of the figure illustrates the creation of an exemplary peripheriness ranking based on the neighborhood coreness (blue numbering): (1) Determine k-shell index for each node; (2) neighborhood coreness is obtained as the sum of all neighbor indices; (3) rank nodes in ascending order of neighborhood coreness. Finally, endangerment ranking and peripheriness ranking are compared.

while the equation for the abundance of an animal species A_j can be written in the same way by interchanging P and A. In the model, the vector $\mathbf{P}$ holds the state variables corresponding to the abundances of all N_P plant species P_i ($i = 1, \ldots, N_\mathrm{P}$) and the vector $\mathbf{A}$ holds the abundances of all N_A animal species A_j ($j = 1, \ldots, N_\mathrm{A}$).

A species' intrinsic dynamics f_i constitute the dynamics which are independent of any other species, with

$$f_i(P_i) = \alpha_i - \beta_{ii}^\mathrm{P} P_i \,. \tag{2}$$

In order to obtain multistability [42], we assume the benefit a species gains from mutualistic interactions (the pollination process) to be obligatory for its own growth and thus we choose the intrinsic net growth rate $\alpha \leqslant 0$. The strength of the intraspecific competition between individuals of the same species is given by the parameter β_{ii}^P.

In addition to intraspecific competition, we include the interspecific competition g_i between species from the same class of species (or guild) – plants compete with plants and animals with animals (intra-guild competition) – with

$$g_i(\mathbf{P}) = \sum_{l \neq i}^{N_\mathrm{P}} \beta_{il}^\mathrm{P} P_l \,. \tag{3}$$

In the case of plant species, β_{il}^P holds the competitive pressure of plant species l on plant species i.

Ultimately, the plant–pollinator network (e.g. figure 1(a)) is built by the mutualistic interactions. In the most commonly applied formulation—introduced in [6]—the mutualistic benefit m_i a species obtains from its partners saturates in accordance with a Holling type II functional response

$$m_i(\mathbf{A}) = \frac{\sum_{j=1}^{N_\mathrm{A}} \gamma_{ij}^\mathrm{P} A_j}{1 + h \sum_{j=1}^{N_\mathrm{A}} \gamma_{ij}^\mathrm{P} A_j} \,, \tag{4}$$

where the parameter h describes the handling time and γ holds the topology of the mutualistic network and the strength of the involved interactions. The mutualistic network is bipartite and thus the mutualistic

benefit of plant species i depends on the abundance of the animals A_j it interacts with (inter-guild mutualism). More specifically, γ_{ij}^{P} gives the relative benefit plant species i obtains from animal species j. In accordance with former studies [24, 25], we assume that this relative benefit depends on a species' degree of specialization, which is expressed by the following trade-off

$$\gamma_{ij} = \gamma_0 \frac{\delta_{ij}}{k_i^{\zeta}}\,, \tag{5}$$

where γ_0 is a constant capturing the general mutualistic strength, $\delta_{ij} = 1$ if species i and j are linked and $\delta_{ij} = 0$ if they are not, k_i is the number of links species i has and ζ specifies the strength of the trade-off ($\zeta \in [0, 1]$, with no trade-off for $\zeta = 0$ and full trade-off for $\zeta = 1$).

Except for the Allee effect $q(P_i)$, equations (1)–(5) correspond to a commonly used formulation of a mutualistic system (e.g. [6, 10, 25, 31, 44, 46, 47]). The Allee effect describes the phenomenon that a small abundance can adversely affect a species' own per-capita growth [48]. Pollinators and pollinated plants are both likely to be subject to such an effect due to, e.g. inbreeding depression, pollen scarcity, sterilization due to haplodiplocity, or impaired mate finding or cooperation-based defense strategies [33, 49–51]. We consider a formulation of the Allee effect which affects the mutualism-dependent growth rate and which is often associated with the issue of mate-finding (or, in the case of plants, attracting pollinators)

$$q_i(P_i) = 1 - \exp\left(-\frac{P_i}{\theta_i}\right)\,, \tag{6}$$

where the parameter θ_i controls the strength of the Allee effect. It is important to note that $q_i(P_i) \in [0, 1]$ can only weaken but not reverse the mutualistic benefit ($q_i m_i \geqslant 0$). In combination with the negative intrinsic growth rate α_i, this induces an Allee threshold, which means that a species' overall per capita growth rate becomes negative below a certain critical population size ($\mathrm{d}P_i/\mathrm{d}t < 0$ for $P_i < P_i^{\mathrm{crit}}$). This ultimately ensures that the system has a sufficiently high number of coexisting stable states.

2.2. Extinction probability and endangerment rank

The premise of this study is that the dynamical system of plants and pollinators exhibits multistability and that one desired state $\mathbf{X_0}$ (figures 1(a) and (b)) in which all species coexist competes with multiple undesired states in which some species are lost or extinct (e.g. $\mathbf{X_a}$ in figures 1(b) and (c)). Accordingly, a perturbation in state variables can induce the loss of species if it pushes the system state into the basin of attraction of an undesired state (figure 1(b)). Our aim is to assign an endangerment score and rank to each species in light of such perturbations. For simplicity, we consider random instantaneous perturbations which we apply by drawing the initial abundance of each species from a uniform distribution within the interval $[0, N_i^*]$, where N_i^* is the abundance of species i in the desired steady state $\mathbf{X_0}$. The ultimate effect of a perturbation is evaluated by numerically integrating [52] the system until it reaches its final stationary state, which can be the desired or an undesired state.

In the end, we determine the endangerment ranking in four steps (see figure 2(a)): (1) We numerically determine the desired state $\mathbf{X_0}$ of the system. (2) We perturb $\mathbf{X_0}$ a number of times N_Δ and determine the corresponding final stationary states. (3) For each species i, we count in how many L_i of the approached states it is extinct, and obtain the extinction probability as $\Omega_i = L_i/N_\Delta$. (4) We then rank the species according to their extinction probabilities Ω from most to least endangered, where the species with the highest Ω_i obtains the rank 1.

2.3. Centrality metrics and ranking algorithms

Topological ranking algorithms or centrality metrics usually aim at sorting nodes of a network according to their 'importance', often with an emphasis on identifying particularly important nodes [53, 54]. In this work, we test different ranking algorithms with regard to their ability to rank nodes of mutualistic networks in accordance with the endangerment of the corresponding species (see figure 2). Since we assume that the most endangered species are located in the network periphery, we always rank the species from most to least peripheral (or from least to most central) and refer to the obtained sorting as peripheriness ranking (see figure 2(b)). In general, we aim for metrics that are ecologically meaningful and easy to interpret.

Degree: The simplest measure of centrality is the *degree* (k), which is defined as the number of links a node has. An advantage of the degree is that it is easy to access and interpret. For example, in a mutualistic network of plants and pollinators, the degree is equivalent to the degree of specialization of species. Since the particular endangerment of specialist species has been emphasized by multiple empirical studies, the degree might be a suitable starting point for linking network topology and endangerment.

Iterative refinement: However, the degree is a purely local metric that neglects the importance or centrality of neighbors. In a mutualistic system, each species depends on partner species, which in turn rely on further other partners, which makes networks of mutualistic interdependencies prime examples of mutual reinforcement. Iterative refinement metrics such as the *eigenvector centrality* (EV) [55] consider this aspect as they assign each node a score which depends on the number and scores of its neighbors. Due to its self-referential definition, which reads

$$\mathbf{x} = \kappa^{-1}\mathbf{B}\mathbf{x}\,, \tag{7}$$

the eigenvector centrality $\mathbf{x}$ takes into account the whole network structure—contained in the adjacency matrix $\mathbf{B}$. In this notation, the constant κ corresponds to the largest eigenvalue of $\mathbf{B}$.

One disadvantage of the eigenvector centrality is that it tends to accumulate in a few nodes. In order to avoid this, we introduce a saturation to the eigenvector centrality

$$\mathbf{x} = \frac{\mathbf{B}\mathbf{x}}{1 + h_e\mathbf{B}\mathbf{x}}\,. \tag{8}$$

The chosen saturation is in line with the typical formulation of the mutualistic benefit, which is often described by a Holling type II functional response (see equation (4)). In reference to the Holling type, we call this centrality index the *eigenvector centrality type II* (EV2). In accordance with equation (4), the parameter h_e corresponds to the handling time. For the sake of simplicity, we set $h_e = 1$ throughout this work.

k-shell index: An alternative and simple approach for considering a node's position within the potentially hierarchical structure of a network is the k-shell decomposition [22], which assigns a *k-shell index* (k_s) to each node (see section 1). In fact, since mutualistic networks possess a core-periphery structure which has been shown to be essential for their structural integrity [23], a ranking considering the coreness (or peripheriness) of a node might be worthwhile.

k-shell refinement: Because many nodes are assigned to the same shell, the k-shell decomposition is fairly limited when used to rank all nodes of a network (see left side of figure 2(b)). However, in plant–pollinator networks, which typically include many specialists, the same is true for the degree. Fortunately, owing to its generally good performance, especially in capturing influential spreaders [56], multiple adaptations of the k-shell decomposition have been proposed (e.g. [57–60]). All of these adaptations provide an improved resolution concerning the distinction of nodes.

In this work, we apply two of these adaptations. The first is the *neighborhood coreness* (C_{nc}) [58], which is obtained by simply summing up the k-shell indices of a node's direct neighbors Λ_1

$$C_{\mathrm{nc}} = \sum_{j\in\Lambda_1} k_s(j)\,. \tag{9}$$

Importantly, this yields an index which combines the degree of a node with the coreness of its neighbors—a rather basic approach to combine connectedness with position. In figure 2(b), this index is used to demonstrate the general procedure to obtain a peripheriness ranking.

The second adaptation—the *neighborhood centrality* (C_{N}) [61]—is slightly more elaborated but still intuitively interpretable (see below). It is defined as

$$C_{\mathrm{N}} = \sum_{r=0}^{R}\left(d^r\sum_{j\in\Lambda_r}\theta_j\right)\,, \tag{10}$$

where θ is the benchmark centrality (in our case, the k-shell index) and Λ_r is the set of nodes whose distance to node i equals r. The parameter R denotes the range of neighborhood which is taken into account, i.e. for $R = 1$, only a node's direct neighbors are considered, for $R = 2$, also the next order neighbors and so on. The parameter d controls the diminishing impact of nodes in the neighborhood of node i with increasing distance to node i. According to Liu *et al* [61], d should be in the range $[0, 1]$.

Using the k-shell index as the benchmark centrality and setting the parameter d to an arbitrary but very small value ($d = 0.001$) allows an instructive interpretation of the neighborhood centrality. For $d \ll 1$, the rank of a node is primarily based on its own k-shell ($r = 0$), while the sum of the k-shell indices of its neighbors is a secondary argument ($r = 1$), the sum of the k-shell indices of its second-order neighbors a tertiary argument ($r = 2$) and so on (we set $R = 2$ and thus only consider primary, secondary and tertiary arguments). Due to this hierarchical configuration of arguments (most, second most, third most important),

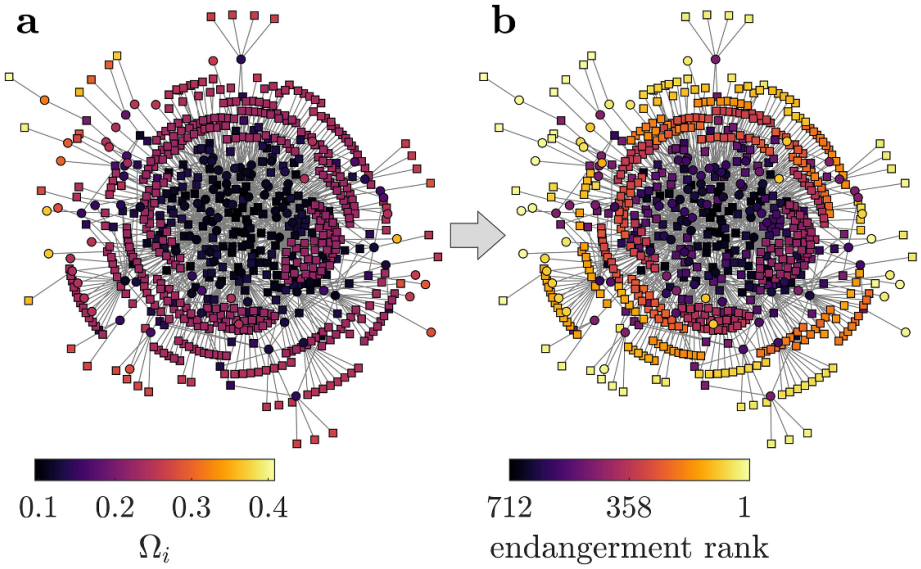

Figure 3. Endangerment of species within an exemplary network. (a) Extinction probabilities Ω of species. (b) Endangerment ranks of species. Squares depict animals and circles plants. Parametrization corresponds to the standard setup with competition type I (see appendix B). Placement of the vertices is based on the Kamada–Kawai algorithm [63].

the neighborhood centrality highlights nodes within tree-shaped structures. In fact, since both their own and the k-shell indices of their neighbors are 1, nodes in the outermost positions of tree-shaped structures obtain the lowest centralizes.

3. Species in trees are most endangered

Now that we have established the necessary tools for creating endangerment and peripheriness rankings, we are set to examine how the two relate. Accordingly, what follows is the centerpiece of this work, in which we present how the core-periphery structure of mutualistic networks affects the simulated endangerment of species.

3.1. Exemplary endangerment ranking

First, we consider an exemplary mutualistic system (figure 3) which stems from a plant–pollinator network on the Amami Islands in the Ryukyu Archipelago, Japan [62] (M_PL_044 in table A1). To start with, we set up the dynamical system according to the standard parametrization (see section 2.1 and appendix B) and numerically determine the desired state in which all species coexist ($P_i^* > 0 \,\forall\, i$ and $A_j^* > 0 \,\forall\, j$). Based on this pre-disturbance state, we then calculate the extinction probabilities Ω for all species and derive the corresponding endangerment ranking (according to the explanations in figure 2(a) and in section 2.2 with $N_\Delta = 5 \times 10^5$).

Already the visual inspection of Ω (figure 3(a)) suggests the conclusion that the degree of specialization and its position within the core-periphery structure determine a species' endangerment. Especially a low degree, which corresponds to a high level of specialization, seems to establish a species' status as being endangered. However, the endangerment ranking (figure 3(b)) indicates that the core-periphery structure shapes the endangerment ranking of species as well. We find that specialists close to the core hold a lower endangerment rank than species in the outer parts of the network (according to the Kamada–Kawai visualization). Moreover, we find that the most endangered species are those in the outermost positions of tree-like structures (*bees in trees*).

3.2. Peripheriness vs. endangerment rankings

In the following, we compare the endangerment rankings to rankings based on different centrality metrics (see section 2.3 and figure 2(b)) for a set consisting of 11 of the largest plant–pollinator networks, including the exemplary network, from the web of life database (see appendix A). However, we sort species from least to most central (reversed centrality or peripheriness rankings) as we assume the correlation between centrality and endangerment to be negative (e.g. low degree equals high endangerment). Importantly, we do not consider all nodes of a network. There are two reasons for this. First, species with the same set of neighbors are topologically and dynamically equivalent (due to our parametrization, see appendix B). We

therefore only include one node from each set of equivalent nodes in the comparison (e.g. $\tilde{N}_{\mathrm{A}}$ denotes the number of unique animal species). Second, comparing the endangerment of animals and plants is questionable since their competitive terms are separated. We concentrate on the numerically dominant group, the pollinators. However, it should be noted that conducting the same analysis for the plants yields similar results (see appendix C).

To evaluate the goodness of fit of the rankings obtained by different centrality indices and the endangerment in these networks (i.e. to 'compare' endangerment and peripheriness rankings, see figure 2), we propose two measures. The first is Kendall's tau [64], which represents a common tool (e.g. [58–61, 65]) to quantify the overall rank correlation between two metrics x_i and y_i (one being the reversed centrality index and the other the endangerment in our case) based on a pairwise comparison of all nodes. The rank correlation coefficient τ is obtained as

$$\tau = \frac{2}{n(n-1)} \sum_{i<j} \mathrm{sign}\left[\left(x_i - x_j\right)\left(y_i - y_j\right)\right] , \tag{11}$$

where n is the total number of nodes compared and $\mathrm{sign}[z]$ is the sign-function which gives $\mathrm{sign}[z] = +1$ if $z > 0$ and $\mathrm{sign}[z] = -1$ if $z < 0$. Accordingly, for each pair of nodes (node i and node j), it is checked whether both metrics arrange the two nodes in the same order ($(x_i - x_j)(y_i - y_j) > 0$) or not ($(x_i - x_j)(y_i - y_j) < 0$). A value of τ close to 1 means that most pairs are arranged in the same way by the two metrics, which indicates a strong positive correlation between the two rankings. For the purpose of this work, a strong positive correlation shows an overall high accuracy of the proposed peripheriness index in ranking nodes in accordance with the endangerment of the corresponding species.

The second measure is inspired by the imprecision function proposed by Kitsak *et al* [56]. In our adaptation, we compare the average extinction probability $M_{\mathrm{cen}}(\rho)$ of a small fraction $\rho\tilde{N}_{\mathrm{A}}$ $(0 < \rho < 1)$ of all considered nodes/pollinators $\tilde{N}_{\mathrm{A}}$ to the average extinction probability $M_{\mathrm{most}}(\rho)$ of the $q\tilde{N}_{\mathrm{A}}$ nodes with the highest extinction probability Ω_i. It should be noted that if the set is not unique (e.g. due to multiple nodes having the same degree), $M_{\mathrm{cen}}(\rho)$ is calculated as the worst possible realization. The measure is then obtained as

$$\epsilon = \frac{M_{\mathrm{cen}}(\rho) - \Omega_{\mathrm{min}}}{M_{\mathrm{most}}(\rho) - \Omega_{\mathrm{min}}} , \tag{12}$$

where the minimal extinction probability Ω_{min} of all $\tilde{N}_{\mathrm{A}}$ nodes is used as a scaling factor. The closer ϵ is to 1, the better the corresponding reversed centrality index is in correctly capturing the most severely endangered species. Accordingly, we refer to ϵ as the precision function (imprecision would be $1 - \epsilon$, see [56]). The precision function puts special emphasis on a small subset of the ranking (we choose $\rho = 0.05$) which represents the few most endangered species. In this regard, the precision complements Kendall's tau. In figure 4, both measures—τ (angle) and ϵ (radius) – are displayed together.

The degree (blue), the eigenvector centrality (yellow) and the eigenvector centrality type II (orange) all provide at least a decent approximation of the endangerment ranking (figures 4(a)–(d)). However, the results also reveal some significant differences between the three ranking algorithms. First of all, the impression that the degree is a good indicator of a species' endangerment is backed up by the general strong correlation between the rankings (high τ for blue marks in figure 4(d)). Noteworthy is that the strong impact of the degree is in part due to the Allee effect which in combination with large perturbations induces a certain ground-endangerment for every species. As any species can be lost if its own abundance falls below a certain threshold, species with low degree have a much higher chance of losing all partners and thus eventually becoming extinct (see appendix D for an elaborated explanation). However, the degree is not capable of separating the set of the most endangered species (low ϵ for blue marks in figure 4(d)). In fact, the degree only provides a kind of presorting that puts species into certain classes of endangerment (see figure 4(a)).

By contrast, the eigenvector centrality EV (figure 4(b) and yellow marks in figure 4(d)) captures the most endangered species well (high ϵ) but provides a worse overall ranking than the degree (lower τ). Finally, the best agreement with the endangerment ranking is obtained by the eigenvector centrality type II EV2 (figure 4(c) and orange marks in figure 4(d)) which surpasses the other two in both the overall rank correlation (τ) and the capability of identifying the most severely endangered species (ϵ). This is because its own connectivity (degree) and the position of its neighbor(s), which both significantly contribute to the EV2, determine a species' endangerment. The contribution of both aspects can be demonstrated by means of the mutualistic benefit a species obtains right after the initial perturbation, which depends on the number and the pre-disturbance abundance of partner species. As the latter arises from the mutual enforcement between species, it strongly depends on the partners' position within the network (see appendix E for an elaborated explanation).

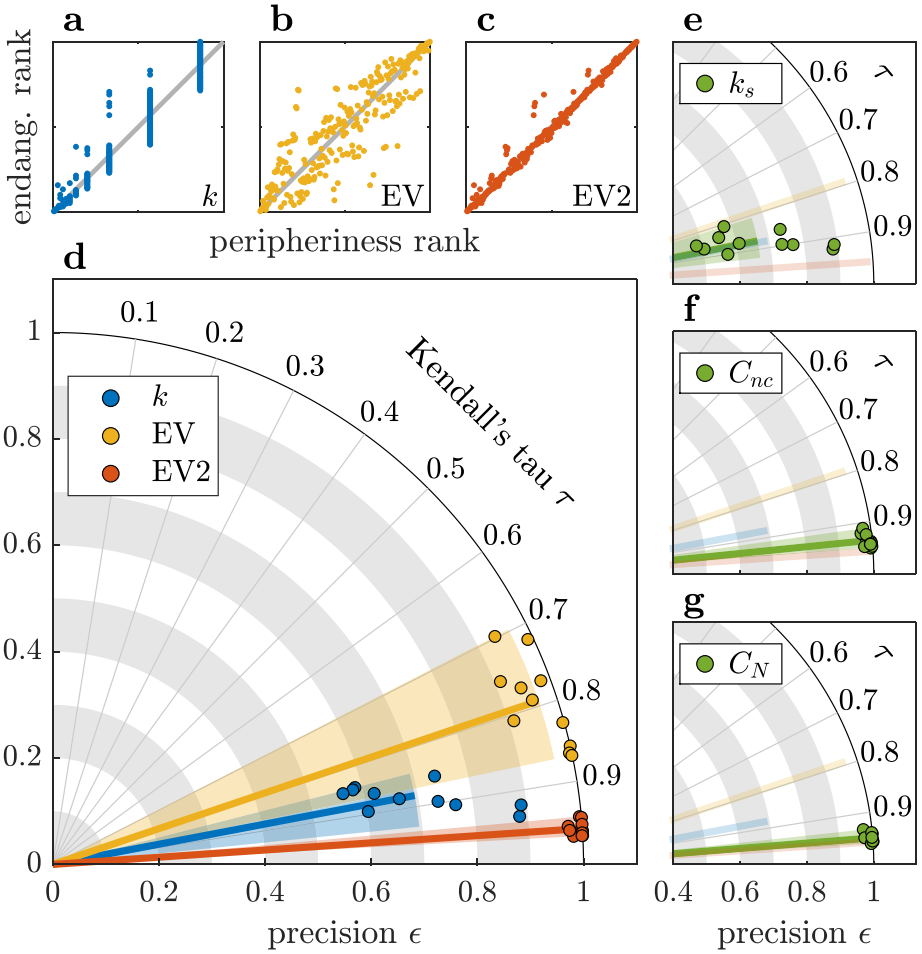

Figure 4. Goodness of fit between node rankings obtained from peripheriness indices (inversed centrality) and simulated species endangerment. (a)–(c) Comparison for one exemplary plant–pollinator network: Peripheriness rank based on degree k (a), eigenvector centrality EV (b) and eigenvector centrality type II EV2 (c) versus endangerment rank. Each point corresponds to one node/species in the network. The closer the points are to the diagonal, the better the agreement between the two rankings. (d)–(g) Comparison for 11 empirical plant–pollinator networks: The evaluation is based on the rank correlation coefficient Kendall's tau τ (angle) and the precision ϵ (radius). Each colored point displays τ and ϵ for the comparison between the species endangerment and one specific peripheriness index for one network. The line displays the mean value of all 11 τ and ϵ and the fan the range of all 11 τ that are obtained based on the same peripheriness index. In (d), the peripheriness indices are based on degree (blue), eigenvector centrality (yellow) and eigenvector centrality type II (orange). In (e)–(g), the peripheriness indices are based on k-shell index k_s (e), neighborhood coreness C_{nc} (f) and neighborhood centrality C_N (all depicted in green). The closer the points (and the tip of the line) are to the bottom right corner where $\tau = 1$ and $\epsilon = 1$, the better the agreement between the two rankings.

In order to obtain a better insight into the correlation between the endangerment of species and the specific core-periphery structure of mutualistic networks, we consider simple measures of the coreness, the k-shell index and two of its variants (see section 2.3). The k-shell index provides a fit similar to the one achieved by the degree, concerning both the rank correlation τ and the precision ϵ (green marks in figure 4(e)). Accordingly, a node's coreness alone does not provide a sufficient explanation for the particular endangerment of some specialists (this is hardly surprising as a node with a degree of 1 is always located in the 1-shell). However, already the simplest adaptation of the k-shell index—the neighborhood coreness C_{nc} (green marks in figure 4(f)), which is obtained as the sum of a node's neighbors k-shell indices—works pretty well (only slightly worse than the EV2). The reason is that this index combines the two aspects which can be shown to be decisive for a species' vulnerability to random shocks, its degree and the coreness of its neighborhood (see appendices D and E). An even better agreement—roughly as good as the EV2 – is obtained by the neighborhood centrality C_N based on the k-shell index (green marks figure 4(g)). As mentioned earlier (see section 2.3), this metric is especially beneficial for the interpretation of our results as it uses a node's own, its first-order neighbors' and second-order neighbors' shell indices as primary, secondary and tertiary arguments and thus highlights nodes which are located deep within tree-shaped and tree-like structures as the least central ones. Accordingly, the good fit between the reversed neighborhood centrality and the endangerment encourages our initial impression that the most endangered species are those in the outermost periphery.

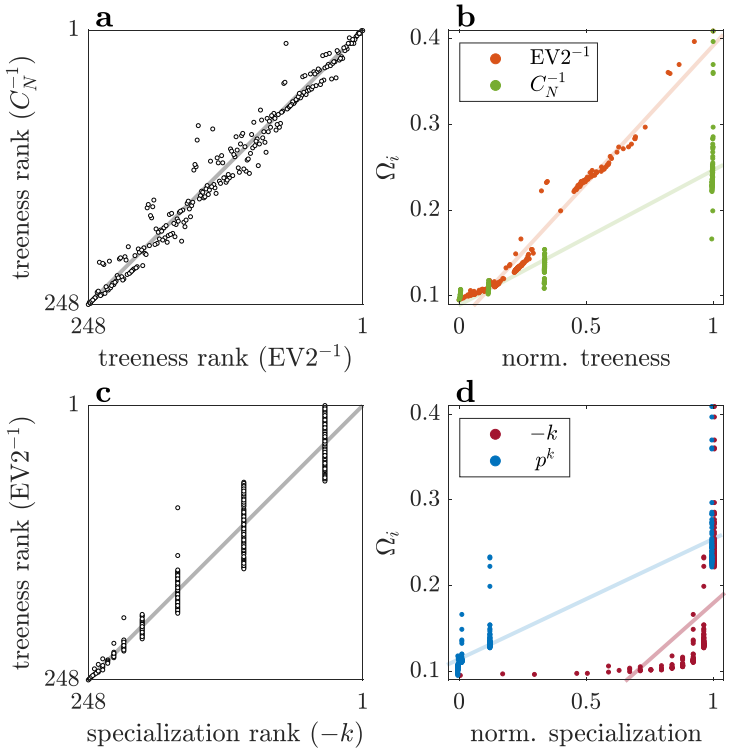

Figure 5. Relation between eigenvector centrality type II (EV2), neighborhood centrality (C_N) and degree (k) within an exemplary network. (a) Correlation between the treeness rankings based on EV2 and based on C_N. (b) Linear correlation between the treeness (normalized to the interval $[0, 1]$) based on EV2 and based on C_N and the extinction probabilities Ω. (c) Correlation between the specialization ranking based on the negative degree $-k$ and the treeness ranking based on EV2. (d) Linear correlation between the specialization (normalized to the interval $[0, 1]$) based on $-k$ and based on the power law description p^k and the extinction probabilities Ω. The parameter p is set as the difference between the lowest Ω_i of all nodes with degree 1 and the overall lowest Ω_i (see appendix D).

3.3. Treeness vs. extinction probability

Both the EV2 and the neighborhood centrality (C_N) capture the endangerment ranking of pollinators exceptionally well. In fact, the rankings obtained by the two algorithms resemble one another (figure 5(a)), which is why, from now on, we refer to both of them as treeness rankings. However, importantly, the underlying distribution of centrality indices (or better treeness indices) shows immense differences. This becomes apparent when looking at the linear correlation between the two indices and the actual extinction probabilities Ω (figure 5(b)). While the block-wise distribution of C_N indices provides only a very broad approximation to Ω, the EV2 – which is based on the Holling type II functional response also used in the dynamical model of the plant–pollinator system (see equation (4)) – captures the distribution of extinction probabilities very well.

An important factor to the great fit between the endangerment described by Ω and the treeness described by the EV2 is that the degree of specialization significantly contributes to the latter metric. In fact, we find that all pollinators which obtain the 69 highest treeness ranks (according to the EV2) have a degree of $k = 1$ (see figure 5(c)). But, in contrast to the EV2 (see figure 5(b)), the degree k shows a very poor linear correlation with the extinction probability Ω (figure 5(d)). The reason is that the impact of the degree on species endangerment is not linear but broadly follows a power law which describes a species' chance of losing all mutualistic partners due to the initial shock perturbation, i.e. $\Omega_i \propto p^{k_i}$ (where the constant p provides some kind of basal-endangerment that is the same for all species; see appendix D for the derivation of this relation based on a simplified model of the mutualistic system). Therefore, in the following, we will use the power law description of the degree p^k as a measure of a species' specialization. As a measure of the treeness, we will use the EV2, since it captures both the endangerment ranking and the distribution of extinction probabilities Ω particularly well.

4. Species in trees are most endangered under different conditions

So far, our findings are based on a single parametrization scheme. However, the chosen parameters are somehow arbitrary and environmental conditions (and thus system parameters) may change. Accordingly, it

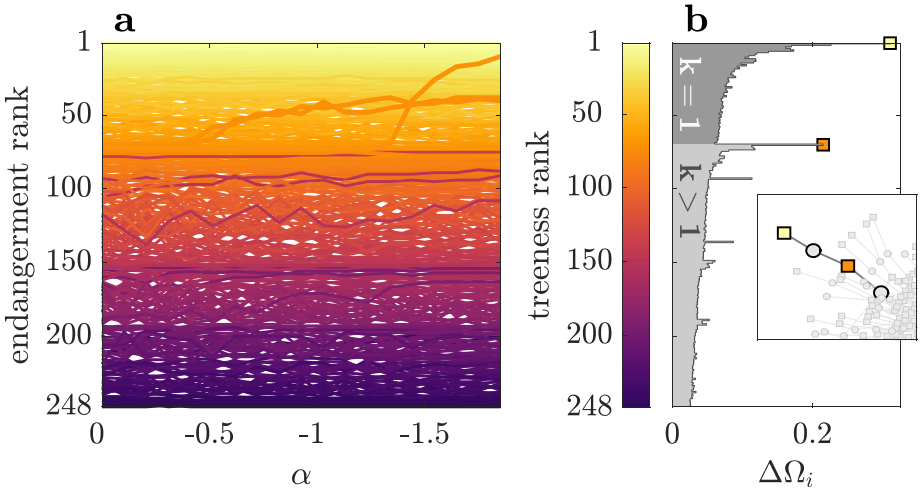

Figure 6. Evolution of the endangerment ranking with increasing stress level. (a) Development of endangerment ranks as the intrinsic growth rate α is decreased from $\alpha = 0$ to $\alpha \approx -1.7$. Color coding of the different species corresponds to treeness rank based on the EV2 of the respective node (see colorbar in the center). (b) Change in extinction probability $\Delta\Omega$ from highest to lowest α, $\Delta\Omega_i = \Omega_i(\alpha \approx -1.7) - \Omega_i(\alpha = 0)$. Species are ordered according to their treeness rank (in line with the axis of the colorbar). Location of two pollinators/nodes (yellow and orange square) with exceptionally high increase in Ω_i is highlighted in the small inset.

is informative to test for the robustness of the obtained rank correlations. To this end, we consider once again the exemplary plant–pollinator network from the Amami Islands (see figure 3) and check how the endangerment of species evolves when an exemplary parameter changes.

4.1. Robustness of the endangerment ranking

First, we check the robustness of the endangerment ranking for the standard system setup (see appendix B). Our parameter of choice is the intrinsic growth rate α, which we assume to be negative and whose further decrease can be interpreted as a globally increasing stress level affecting all species in the same way (e.g. harsher conditions due to anthropogenic impact). We vary α within an interval in which the mutualism remains obligatory ($\alpha \leqslant 0$) and in which the long-term coexistence of all species is possible (the desired state is stable). It should, however, be noted that for the most negative values of α, the system is close to a bifurcation (tipping point) at which some species would inevitable go extinct.

We find that, overall, the endangerment ranking is pretty robust and thus the proposed centrality metrics, like the EV2, provide a good fit for all values of α. This can be seen in the consistent distribution of colors in figure 6(a): Nodes in the core (dark/purple) permanently remain at low ranks, while peripheral nodes (bright/yellow) occupy the upper endangerment ranks. Nevertheless, we do observe that for a few individual nodes the endangerment rank changes significantly—particularly noticeable is a jump of one of the orange-colored nodes from endangerment rank 73 (at $\alpha \approx -1.2$) to rank 10 (at $\alpha \approx -1.7$, figure 6(a)).

In order to better understand this jump and to check whether it might undermine the general validity of our former findings, we take a look at the change in the absolute extinction probabilities $\Delta\Omega$ from the highest to the lowest α (figure 6(b)), $\Delta\Omega_i = \Omega_i(\alpha \approx -1.7) - \Omega_i(\alpha = 0)$. The absolute extinction probabilities Ω do of course adapt to the changing conditions—lower growth rates α generally entail higher extinction probabilities Ω and thus $\Delta\Omega_i > 0$ for all species i. However, the change $\Delta\Omega$ is not evenly distributed across species (figure 6(b)). We find that more peripheral species (higher treeness ranks) tend to show a higher increase in Ω_i than species which are closer to the core (lower treeness ranks). But, there are some clear outliers to this trend. The most obvious of them is the above-mentioned node that jumps from endangerment rank 73 to 10 (marked by an orange square in figure 6(b)). Taking a look a the corresponding node's position in the network (inset in figure 6(b)), we see that its high $\Delta\Omega_i$ can be associated with the node's proximity to the most peripheral (highest treeness) and most endangered (highest Ω_i) pollinator-node in the system. Furthermore, the node is itself located within a tree-structure. Accordingly, this phenomenon does not undermine our former findings since the highest endangerment still originates from the most peripheral species.

4.2. Composite centrality index

What we do observe is that, for α close to 0, the set of the most endangered species only consists of specialists with a degree of $k = 1$ (there are 69 unique species with a degree of 1, all of them are within the set of the 69

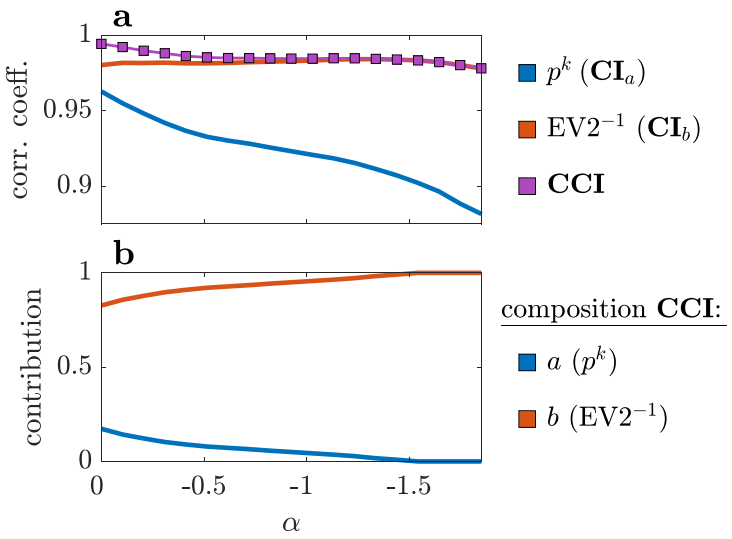

Figure 7. Topological determinants of endangerment for different values of α. (a) Linear correlation between the extinction probability Ω and p^k (blue line), EV2 (orange line) and the best composite centrality index **CCI** (purple squares) which is obtained as the weighted sum of the normalized forms of p^k and EV2^{-1}. (b) Best composition of the **CCI** with a describing the contribution of p^k and b the contribution of EV2^{-1}.

most endangered species). Due to the strong increase in the extinction probability of some species (figure 6), this changes and some nodes with degree $k > 1$ enter the set of the most endangered species as α decreases (i.e. for smaller α, the set of the 69 most endangered species also contains species with $k > 1$).

In fact, by examining the correlation between the extinction probability Ω and the power law p^k, we can see that the degree loses explanatory power as a determinant of species endangerment. For good conditions (greater α), the endangerment of species can well be captured by the power law p^k, i.e. $\Omega_i \propto p^{k_i}$. However, as α is decreased, the correlation coefficient declines (blue line in figure 7(a)). By contrast, the EV2 captures the extinction probability Ω very well for all values of α and only slightly declines for smaller α (red line in figure 7(a)).

Although the EV2 provides a good fit for all values of α, we test whether the degree can add additional explanatory value. To this end, we apply a hybrid method [66] by setting up a composite centrality index

$$\mathbf{CCI} \;=\; a\mathbf{CI}_a + b\mathbf{CI}_b \;, \tag{13}$$

with $a + b = 1$ and $a, b \geqslant 0$. The **CCI** is obtained as the weighted sum of two normalized centrality indices, where $\mathbf{CI}_a$ is the normalized form of p^k and $\mathbf{CI}_b$ the normalized form of EV2^{-1}. The normalization is obtained by setting the length of each vector to 1. To receive the best composition of **CCI**, we then check for each value of α which combination of a and b provides the highest Pearson's linear correlation coefficient with the extinction probability Ω.

Following the best composition of **CCI** (figure 7(b)), we see that the EV2 is the dominant descriptor of the endangerment for all α. For greater α, the EV2 underestimates the explanatory value of the degree and thus a composite which takes a small contribution of the degree provides the highest correlation coefficient with the endangerment. As α decreases, the contribution of the degree vanishes, i.e. the importance of the degree for the overall endangerment decreases.

5. Species in trees are most endangered—but which trees?

Now, after having established that the particular endangerment of mutualistic species in tree-like substructures is rather robust against changes in an exemplary parameter, we shortly illuminate an aspect which might undermine the general validity of this finding: Real plant–pollinator systems are actually multilayer networks. For instance, in addition to mutualistic links with certain plants, pollinators also have antagonistic links to other pollinators with whom they compete for food and/or nesting sites.

Due to the consideration of intra-guild competition (equation (3)), the mutualistic model in principle already considers the multilayer nature of plant–pollinator networks. However, the assumption that all species within one guild compete with all other species in the same guild in a uniform manner (see left side of figure 8(a)) – also called *competition of mean-field type* [6]—represents a strong simplification [67]. Although a realistic topology is difficult to obtain, a reasonable alternative to the mean-field approach is to

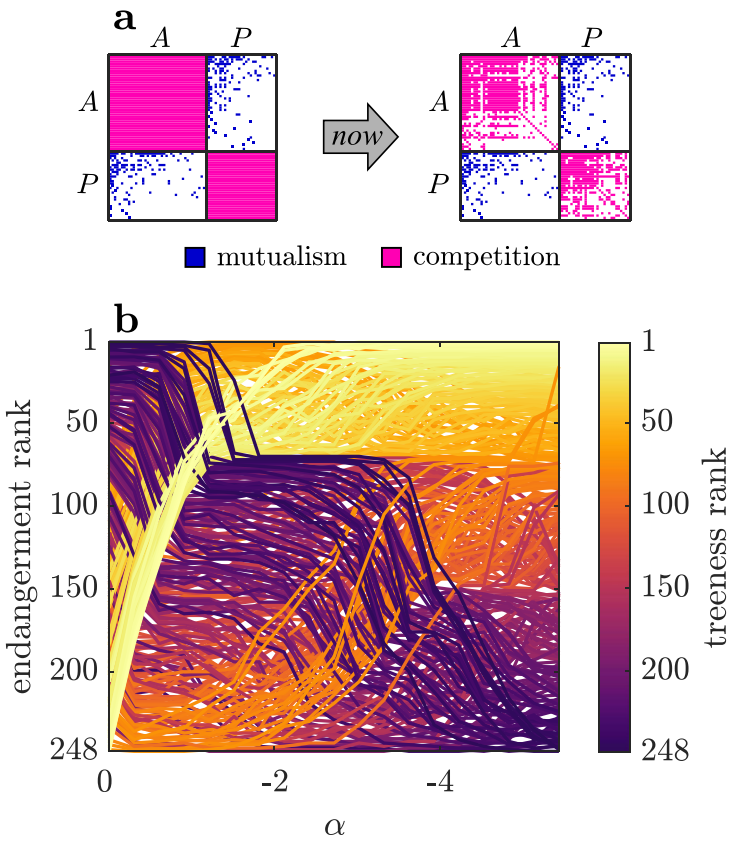

Figure 8. Evolution of the endangerment ranking with increasing stress level for the case of explicit intra-guild competition topologies. (a) So far, we assumed that species competed with all other species from the same guild in a uniform manner (adjacency matrix on the left side illustrates *competition type I*). Now, we consider the case of an explicit competition topology which is based on the assumption that the resources for which species compete are their mutualistic partners (adjacency matrix on the right side illustrates *competition type II*). (b) Development of endangerment ranks as the intrinsic growth rate α is decreased for the mutualistic model with an explicit competition topology. Color coding of the different species corresponds to treeness rank based on the EV2 of the respective node.

assume that the resources for which species compete are their mutualistic partners [67]: Plants compete for pollinators and pollinators for plants. Accordingly, we can derive an explicit competition topology by drawing a competitive link between two species from the same guild if they share a common mutualistic partner. Importantly, this way of constructing the competition topology gives rise to a potential benefit of being located in the periphery of the mutualistic network, since peripheral species tend to obtain fewer competitive links than species which are located in the core of the mutualistic network (i.e. being peripheral allows species to avoid competition). By applying this scheme, we obtain a multilayer network which includes explicit topologies for both inter-guild mutualism and intra-guild competition (see right side of figure 8(a)). In the following, we refer to the corresponding system setup as the *multilayer setup* (*competition type II* in appendix B), in contrast to the *standard setup* (*competition type I* in appendix B) which we considered so far.

5.1. Robustness of the endangerment ranking

Following the same procedure as before (see section 4.1) and using the same exemplary plant–pollinator network (see figure 3), we check how the endangerment of species within the multilayer setup (*competition type II*) changes depending on the intrinsic growth rate α (figure 8(b)). It should again be noted that for the most negative α (right side of figure 8(b)), the system is close to a bifurcation point beyond which the stability of the desired state would no longer be maintained.

It is striking that, under rather stress-free conditions (high α), the obtained endangerment ranking (figure 8(b)) is almost reversed compared to the standard setup (*competition type I* setup in figure 6(a)). As external stress levels increase, first, the endangerment ranks of the most specialized and most peripheral species of the mutualistic layer drastically increase (bright/yellow colored nodes with high treeness ranks take the upper endangerment ranks until $\alpha \approx -2$), followed by the species with intermediate treeness ranks (orange nodes take the medium endangerment ranks until $\alpha \approx -4$). Ultimately, for high stress levels (small α), the endangerment ranking converges towards the ranking which has been obtained for the standard setup (compare right side of figure 8(b) with figure 6(a)).

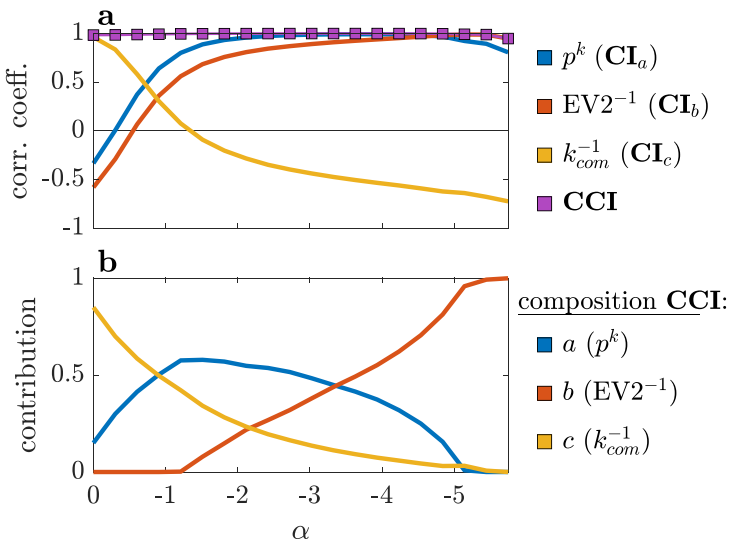

Figure 9. Topological determinants of endangerment in the case of explicit intra-guild competition. (a) Linear correlation between the extinction probability Ω and p^k (blue line), EV2 (orange line), the degree within the competition network k_{com} (yellow line) and the best composite centrality index **CCI** (purple squares) which is obtained as the weighted sum of the normalized forms of p^k, $\mathrm{EV2}^{-1}$ and k_{com}^{-1}. (b) Best composition of the **CCI** with a describing the contribution of p^k, b the contribution of $\mathrm{EV2}^{-1}$ and c the contribution of k_{com}^{-1}.

5.2. Composite centrality index

The evolution of the endangerment ranking (figure 8(b)) indicates that intra-guild competition has a great impact on the endangerment of species when overall conditions are rather favorable (high α) but loses in significance as conditions become harsher (smaller α) – in comparison to the impact of inter-guild mutualism (see also [25]). This impression is backed up by the correlation between the endangerment Ω and a species' degree within its competitive layer k_{com} (figure 9(a)), which is high only for high α and decreases fast as conditions become harsher. In return, the fit between Ω and the two centrality measures referring to the mutualistic layer (p^k and EV2) becomes better as the stress level increases (figure 9(a)). For the most negative α, the best fit with the endangerment is again obtained for the treeness described by the EV2.

We again test whether a composite centrality index **CCI** can provide a good fit for all α. To cover the impact of the competition layer, we expand the index presented in equation (13) by a third normalized centrality index $\mathbf{CI}_c$ and thus obtain

$$\mathbf{CCI} = a\mathbf{CI}_a + b\mathbf{CI}_b + c\mathbf{CI}_c \ , \tag{14}$$

where now $a+b+c=1$ and $a,b,c \geqslant 0$. For the third component $\mathbf{CI}_c$, we use the inverse of the degree k_{com}^{-1} within the competitive layer, i.e. 1 for a pollinator with one competitive link, $1/2$ for a pollinator with two links and so on. We normalize the corresponding vector to a length of 1, so that **CCI** is obtained as the weighted sum of three vectors, each with a length of 1. Again, we check for each value of α which combination of a, b and c provides the highest Pearson's linear correlation coefficient with the extinction probabilities Ω (figure 9(b)). The best **CCI** provides a good fit with the endangerment for all α (figure 9(a)).

Following the best composition of **CCI** with changing α (figure 9(b)), we see how the mutualistic layer replaces the competitive layer as the dominant descriptor of pollinator endangerment. For very high α ($\alpha \approx 0$), the degree within the competition matrix k_{com} is the main driver of the endangerment, while the mutualistic degree only provides a minor contribution. Accordingly, species in tree-like substructures of the mutualistic network are least endangered (see figure 8(b)) – they have few mutualistic partners but also few competitors. On the contrary, species in the core of the mutualistic network are most endangered as the high number of mutualistic partners cannot compensate the impact of having many competitors. With the decrease of α, the impact of k_{com} decreases continuously (figure 9(b)). At first, the contribution of the number of mutualistic partners (p^k) increases in return and becomes the main descriptor of the endangerment for intermediate values of α. As a result, the endangerment of specialists increases dramatically and they replace species in the mutualistic core as the most endangered species (see figure 8(b)). As conditions continue to become harsher, the EV2 becomes a factor (at $\alpha \approx 1.2$). With the increasing impact of the EV2 (figure 9(b)), species in trees establish as the most endangered ones (see figure 8(b)). With the EV2 gradually replacing the mutualistic degree as the main descriptor of the endangerment (figure 9(b)), the endangerment ranking obtained for the multilayer setup (*competition type II*) more and more resembles the

one obtained for the standard setup (*competition type I*) – which means that species in the core are least and species in trees most endangered (see figure 8(b)).

6. Discussion and conclusion

The question how structure affects stability is one of the field-defining questions in ecological network theory. We add a new perspective to this issue by bringing together the concepts of shock-induced tipping [44, 68] and node centrality [69]. To this end, we considered mutualistic plant–pollinator networks as dynamical systems exhibiting multistability, with one desired state in which all species coexist and multiple undesired states in which some species are gone extinct. This implies that an instantaneous state change or shock perturbation can induce a tipping event that causes the loss of some plant and/or pollinator species. For several realistic network topologies, we sorted species from most to least likely to go extinct due to random shock perturbations and compared these endangerment rankings with rankings obtained from network theoretic centrality metrics. In particular, the comparison with three centrality metrics—the degree, an adaptation of the k-shell index and a newly introduced variant of the eigenvector centrality—helped us unravel how the vulnerability of species is shaped by their degree of specialization and by the core-periphery structure of mutualistic networks, with the most endangered species being specialists (nodes with low degree) in the outer periphery (outer k-shells). Particularly well established instances of such peripheral areas are tree-shaped structures of the network which stem from links between nodes/species in the 1-shell (hence the title *'keep the bees off the trees'*).

The particular significance of a pollinator species' degree of specialization for its endangerment has already been highlighted in earlier empirical studies [15, 70]. Furthermore, recent theoretical work demonstrated that the positioning within the core-periphery structure of a mutualistic network can be an important factor for a species' endangerment [23]. Our work affirms such findings but adds a new perspective to the existing theoretical analyses. So far, studies which involved a dynamic description of a plant–pollinator network often examined the system's response to gradual environmental degradation [23, 25–29, 31]. Our work complements such studies by capturing another section of the spectrum of potential stressors. The abrupt and large shock perturbations, which we consider, can be interpreted as non-specific extreme events—a class of disturbances which plants and pollinators are likely to experience (e.g. due to wildfires, extreme rainfall or sudden pesticide exposure). Another difference to most former studies is that, instead of highlighting the point of collapse (i.e. the loss of most or a significant amount of species) or the precursory signs thereof [29, 32], we consider all possible outcomes of a perturbation (i.e. all coexisting attractors), including major as well as minor extinction events.

It is this approach which allowed us to distinguish all pollinator species within a mutualistic network based on their individual chance of getting extinct. The derived endangerment ranking then enabled us to examine how topological traits of nodes might affect the endangerment of corresponding species. In this regard, the finding that topology-based metrics which reflect the 'treeness' of a node—in particular, the inverse EV2 and the inverse neighborhood centrality based on the k-shell index (C_{N}) – are well suited to capture the overall distribution of vulnerabilities is instructive in multiple ways. In particular, it highlights the potential endangerment of species engaging in mutually specialized interactions (species in trees). This might not only concern the endangerment of currently present pollinator species but could also give a hint at why corresponding motifs, like tree-like substructures, are rather rare in plant–pollinator networks. Another aspect refers to the usual use of the applied ranking algorithms. Centrality metrics, like the eigenvector and neighborhood centrality, have been developed to identify the most important nodes within networks. Accordingly, losing the most endangered species, corresponding to the nodes with the lowest centrality (or the highest inverse centrality), is unlikely to profoundly affect the overall network integrity (see also [71]). While this is certainly no bad news, it also implies that many species could be lost long before a mutualistic network is anywhere close to a system collapse—i.e. many species could be extirpated without warning.

The main focus of this work was examining the impact of network topology on species endangerment. We therefore chose a simple parametrization scheme which ensures that species solely differ on account of their position within the mutualistic network. This also meant neglecting multiple phenomena which occur in real plant–pollinator networks, like phenological dynamics which affect the topology of mutualistic networks over the course of a season [11, 21], the spatial configuration of the landscapes that harbor the mutualistic systems [34, 72, 73] or differences in the level of reliance on mutualistic partner species [12, 74, 75] (e.g. some pollinators also feed on resources outside the mutualistic network), to name but a few. Due to the simplistic approach, it should be obvious that our findings cannot be directly applied to assess the endangerment of real world pollinator species. In fact, under certain conditions, the mutual specialization might have had benefits for the involved species, enabling the evolution and persistence of this phenomenon. To shed some light on potential benefits of being located in the periphery, we considered an explicit topology

for the intra-guild competition (switch from *standard setup* to *multilayer setup* in section 5) based on the assumption that the resources for which species compete are their mutualistic partners [67]. We found that being peripheral can be beneficial when conditions are good, since it allows pollinators to avoid competition for resources. However, we also saw that, under comparatively harsh conditions, pollinators in tree-like structures are again the ones being most endangered—i.e. with increasing stress, mutualism rather than competition becomes the decisive interaction for a species' survival (in agreement with the *stress-gradient hypothesis* [76, 77]). A more detailed analysis of the impact of environmental conditions on the variability of the observed vulnerability patterns, for example via a more elaborated sensitivity analysis [78], is a promising task for future research.

In the real world, the multilayer nature of plant–pollinator systems goes way beyond the two layers which we considered in this work. For instance, bees require both nectar and pollen which they often receive from different flowers [79]. Accordingly, a degree greater than 1 does not necessarily mean that a species is not specialized in one way or the other. The same holds true for competition since species do not only compete for mutualistic partners but also for nesting sites (pollinators), and nutrients and space (plants). Overall, we believe that the interplay as well as potential trade-offs between different network layers are aspects which deserve further investigation in future studies. The approach which we presented in this work—creating endangerment/vulnerability scores and comparing them to network-based centrality metrics—can be an instructive tool for such analyses. For further analyses, the tools that we used for the comparison (correlation coefficients and composite centrality indices) could also be replaced, for example, by techniques that enable the consideration of a nonlinear relation between centrality and vulnerability scores (e.g. nonlinear regression). In this way, the approach could also be further developed for use in more realistic settings, for instance, in system setups where species differ on account of intrinsic parameters (like α_i) and on account of their position in the mutualistic network.

Furthermore, our approach can easily be adopted for other fields of application. For instance, the comparison between centrality and vulnerability scores would also be insightful for other networked systems that exhibit multistability. Particularly suitable are networks where the single components can switch between two (or more) alternative states, for instance, power grids, where network elements can be either functional or non-functional [80] or, generally, networks consisting of multiple interlinked tipping elements [81]. Another interesting field of application are other, potentially more complex, disturbance scenarios like periodically recurring disturbances [82], disturbances with an explicit temporal structure [83] or combinations of gradual environmental degradation and shock perturbations [84]. In this context, the use of centrality metrics can also help to examine potential trade-offs between a species' vulnerability against different types of perturbations. For instance, Suweis *et al* [85] found that the impact of small perturbations tends to accumulate in the most central rather than the most peripheral species of mutualistic networks. Further analyzing the relation between topological traits and different aspects of a species' vulnerability in the same system setting is a promising direction for future studies.

Data availability statement

No new data were created or analysed in this study.

Acknowledgment

The simulations were performed at the HPC Cluster CARL, located at the University of Oldenburg (Germany) and funded by the DFG through its Major Research Instrumentation Programme (INST 184/157-1 FUGG) and the Ministry of Science and Culture (MWK) of the Lower Saxony State.

Appendix A. Plant-pollinator networks

The topologies of all studied plant–pollinator networks have been taken from the Web of Life database (www.web-of-life.es). In order to attain a set of comparable, connected networks of sufficient size, we processed the original data as follows: (1) All networks are considered as being unweighted. (2) From each dataset, only the largest connected component is taken while all other components are omitted. (3) Only those networks which hold more than 100 topologically unique pollinator nodes $\tilde{N}_{\mathrm{A}}$ (i.e. nodes which have a unique set of neighbors) are considered—so that we end up with a set of 11 networks (see table A1). The reason for the last selection criterion is that we do not consider all but only the distinguishable nodes for the endangerment and centrality rankings (see section 3.2).

Table A1. Overview of the dataset of applied plant–pollinator (*P-A*) networks. From each dataset only the largest connected component is considered. For the ranking only the unique pollinator nodes ($\tilde{N}_A$) are taken into account.

ID[a]	source[b]	#links[c]	N_P / N_A[d]	$\tilde{N}_P$ / $\tilde{N}_A$[e]
M_PL_005	[86]	918	91 / 270	88 / 170
M_PL_015	[87]	2930	130 / 663	128 / 476
M_PL_021	[88]	1192	90 / 676	79 / 206
M_PL_044	[62]	1121	107 / 605	103 / 248
M_PL_048	[89]	671	30 / 236	30 / 132
M_PL_049	[90]	590	37 / 225	37 / 118
M_PL_053	[91]	567	92 / 272	88 / 139
M_PL_054	[92]	763	106 / 308	101 / 167
M_PL_055	[93]	427	61 / 192	56 / 117
M_PL_056	[94]	871	91 / 365	89 / 188
M_PL_057	[95]	1920	114 / 883	107 / 319

[a] In the web of life database (www.web-of-life.es).
[b] Original study in which the network topology was established.
[c] # mutualistic links in the largest connected component.
[d] # plant/pollinator species in the largest connected component.
[e] # unique plant/pollinator species (considered in the ranking).

Appendix B. Dynamical model set-up

For the choice of parameters in the model of plant–pollinator networks (see section 2.1), two considerations were decisive. The first refers to the main goal of this work, which is to link topological traits of network nodes to the endangerment of corresponding species. To ensure that differences in the endangerment (given by Ω) actually reflect differences in the topological traits of the respective nodes, we choose a parametrization which makes sure that species solely differ on account of their position within the mutualistic network. This is achieved by using the same set of constant parameters for each species i (e.g. $\alpha_i = \alpha \; \forall \; i$). The second important consideration concerns the existence (and attractiveness) of the desired state $\mathbf{X_0}$ in which all species coexist. Since $\mathbf{X_0}$ serves as the ground state for the applied perturbation scheme, which means that the system resides in this state prior to a shock perturbation (see section 2.2), the desired state $\mathbf{X_0}$ should be locally attractive (linearly stable) for each of the examined mutualistic systems (see table A1). We choose the parameters accordingly, with the standard setting being $\alpha = 1.0$, $\beta_{ii} = 1.0$, $\gamma_0 = 10.0$, $h = 0.1$ and $\zeta = 0.5$ (with α being the only parameter which is varied within this work, in sections 4 and 5). Aside from these parameters, the parametrization of the interspecific competition and the parametrization of the Allee effect deserve special consideration (see below).

Competition type I—standard setup: Through most of this work (sections 3 and 4), we stick to the commonly applied *competition of mean-field type* [6]. In this approach, it is assumed that each species within one guild competes with every other species in the same guild in a uniform manner, i.e. every pollinator competes with every other pollinator and every plant with every other plant (see left side of figure 8(a)). To obtain a stable desired state $\mathbf{X_0}$ for networks of different size (see table A1), we assume that the strength of competition between two species is mitigated in accordance with the total number of competitors within the network—i.e. $\beta^P_{il} = \beta_0/(N_P - 1)$ for $i \neq l$ ($\beta^A_{jo} = \beta_0/(N_A - 1)$ for $j \neq o$), where N_P and N_A are the total number of plant and pollinator species in the network and $\beta_0 = 1.5$.

Competition type II—multilayer setup: In section 5, we consider an alternative competition topology (see right side of figure 8(a)) which we derive from the network of mutualistic interactions in the following manner: A competitive link is drawn between two distinct species ($i \neq l$) from the same guild if they share at least one mutual partner ($\beta_{il} > 0$), otherwise no link is drawn ($\beta_{il} = 0$). For the sake of simplicity, we assume that the strength of competition is the same for every pair of competing species—i.e. either $\beta_{il} = 0$ or $\beta_{il} = 0.001$ for $i \neq l$ (applies to both plant competition β^P and pollinator competition β^A).

The Allee effect: Species with lower abundance P_i^* (A_j^*) in the desired state $\mathbf{X_0}$ generally have a higher chance of obtaining a low absolute abundance $P_i(t = 0)$ ($A_j(t = 0)$) after the shock perturbation (see section 2.2). Since the Allee effect q_i depends on the species abundance P_i (see equation (6)), species with low P_i^* would be disproportionately penalized if we would use the same θ_i for all species i. In order to avoid this, we derive an individual θ_i for every species i which depends on the species' abundance P_i^* in the desired state. To achieve this, we divide the parametrization into two stages. In the first stage, we set up a provisional system without

an Allee effect (corresponds to setting $q_i = 1$ for all i) and numerically determine the corresponding provisional desired state $\tilde{\mathbf{X}}_\mathbf{0}$. In the second stage, we obtain θ_i as

$$\theta_i = \frac{-0.1\tilde{P}_i^*}{\ln(0.5)}, \tag{B.1}$$

where $\tilde{P}_i^*$ is the abundance of species i in the provisional desired state $\tilde{\mathbf{X}}_\mathbf{0}$. Since $\tilde{P}_i^* \approx P_i^*$, the Allee effect q_i now depends on a species' relative abundance P_i/P_i^* (insert equation (B.1) into equation (6)). Due to the choice of θ_i, q_i takes a value of 0.5 when species i is at 10% of its abundance P_i^* in the desired state.

Appendix C. Peripheriness vs. endangerment rankings for plants

For the sake of completeness, we conducted the same analysis for comparing endangerment rankings and different peripheriness rankings, as outlined in section 3.2, for the plant species as well. The only difference between the results presented in figure 4 and the ones in figure C1 is that, in the latter, the unique plant species instead of the unique pollinator species are considered (see appendix A for information on the networks considered).

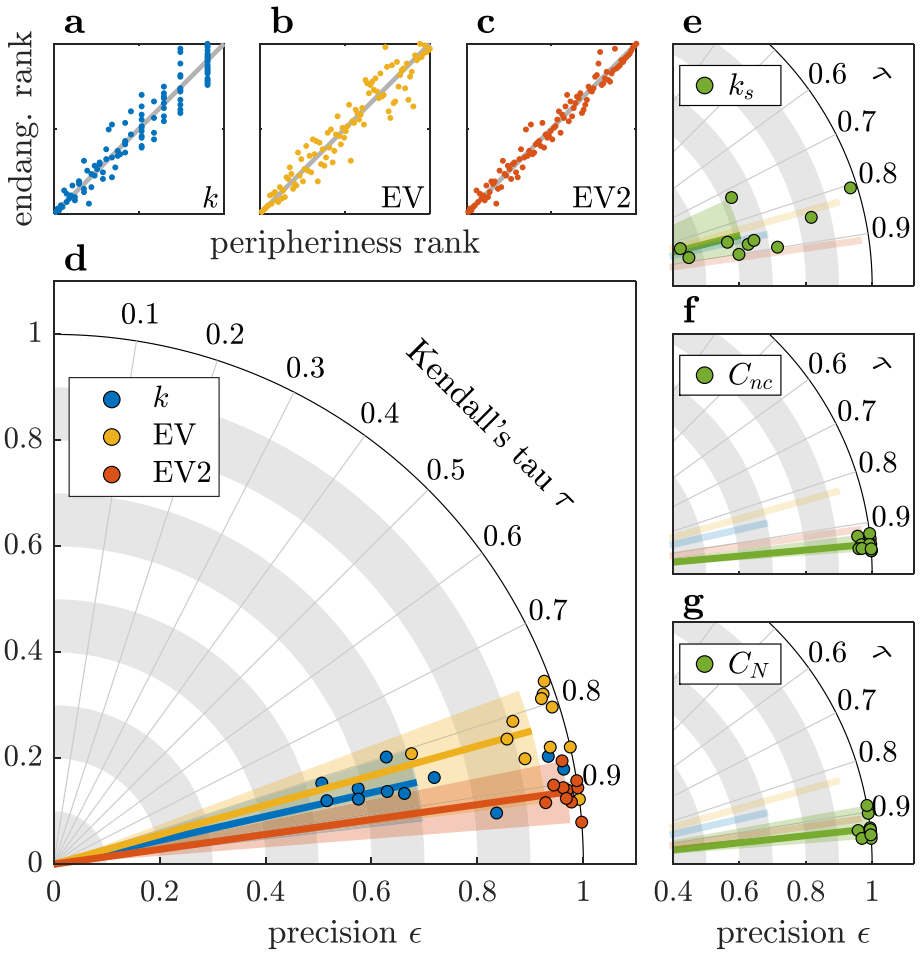

Figure C1. Goodness of fit between node rankings obtained from peripheriness indices (inversed centrality) and simulated species endangerment for the plant species. (a)–(c) Comparison for one exemplary plant–pollinator network: Peripheriness rank based on degree k (a), eigenvector centrality EV (b) and eigenvector centrality type II EV2 (c) versus endangerment rank. Each point corresponds to one node/species in the network. The closer the points are to the diagonal, the better the agreement between the two rankings. (d)–(g) Comparison for 11 empirical plant–pollinator networks: The evaluation is based on the rank correlation coefficient Kendall's tau τ (angle) and the precision ϵ (radius). Each colored point displays τ and ϵ for the comparison between the species endangerment and one specific peripheriness index for one network. The line displays the mean value of all 11 τ and ϵ and the fan the range of all 11 τ that are obtained based on the same peripheriness index. In (d), the peripheriness indices are based on degree (blue), eigenvector centrality (yellow) and eigenvector centrality type II (orange). In (e)–(g), the peripheriness indices are based on k-shell index k_s (e), neighborhood coreness C_{nc} (f) and neighborhood centrality C_N (all depicted in green). The closer the points (and the tip of the line) are to the bottom right corner where $\tau = 1$ and $\epsilon = 1$, the better the agreement between the two rankings.

The results for the plant species (figure C1) look qualitatively similar to the ones for the pollinators (figure 4), although there are some minor differences that can be attributed to the overall smaller number of plant species (see table A1) and to the slightly different distribution of plants within the mutualistic networks (e.g. fewer specialists). As for the pollinators (figure 4(d)), degree (blue), eigenvector centrality (yellow) and eigenvector centrality type II (orange) all show a good agreement with the endangerment ranking, with the EV2 achieving the best fit out of those three (figure C1(d)). Overall, the best approximation of the plant endangerment is provided by the two variants of the k-shell index, the neighborhood coreness C_{nc} (figure C1(f)) and the neighborhood centrality C_{N} based on the k-shell index (figure C1(g)). Accordingly, the peripheriness of species/nodes is a good estimator for plant endangerment as well.

Appendix D. Allee effect induces degree-dependence

In the following, we demonstrate that if we assume that mutualism is obligatory ($f_i < 0$) and that any species can go extinct if perturbed strong enough (Allee effect q_i), a dependence of the endangerment on the degree is inherent in the model of mutualism (equation (1)). To this end, we reduce the model to the necessary ingredients allowing for an extinction threshold and obligatory mutualism. As a first step, we neglect the interspecific competition, $g_i = 0$. Moreover, we assume that a species obtains the full mutualistic benefit as long as it has any partner species left. This effectively reduces the mutualistic benefit m_i to an ON–OFF function which reads

$$m_i = \begin{cases} \text{const} & \text{if any } \gamma^{\mathrm{p}}_{ij} A_j > 0 \\ 0 & \text{else.} \end{cases} \tag{D.1}$$

It should be noted that this form of m_i can be obtained by assuming an extremely efficient mutualism, $\gamma_0 \to \infty$, in which case the constant in equation (D.1) is h^{-1}.

Under the assumption that we only consider connected networks, the extinction of a species in this simplified model can initially be induced only due to its own density falling below the Allee threshold. Further extinctions can occur if a species loses all its partners due to such initial extinction events. Accordingly, the extinction process following a single large shock perturbation can be reformulated by two simple probabilistic rules which denote primary and secondary extinctions.

(1) Primary extinctions: Each species has a probability p_i of going extinct due to the shock.
(2) Secondary extinctions: After the initial shock, species which remain without any mutualistic partner are lost as well. The probability for this to occur is the product of the primary extinction probabilities p_j of the neighbors Γ_i of species i.

Accordingly, the probability of species i to go extinct due a single shock perturbation can be denoted as

$$\Omega_i = p_i + (1 - p_i) \prod_{j \in \Gamma_i} p_j \,. \tag{D.2}$$

For the sake of simplification and in accordance with the parametrization of the Allee effect (see appendix B), we assume that the probability of falling below the primary extinction threshold is the same for all species and thus $p_i = p \; \forall \; i$. This allows us to derive an analytic solution for the extinction probability for each species which solely differs in terms of a species' degree k_i

$$\Omega_i = p + (1 - p)\, p^{k_i} \,. \tag{D.3}$$

Accordingly, in this simple model, each species holds a certain basal-endangerment p, which yields the minimum for the Ω_i of any species, and an additional endangerment term, whose contribution to Ω_i decreases with increasing degree k_i according to the power law p^{k_i}.

In the following, we test whether the extinction probabilities Ω calculated for the complete dynamical model generally follow the dependency described by equation (D.3). To this end, we need to derive a basal-endangerment p for the simplified model (equation (D.3)) based on the extinction probabilities obtained for the complete model. We determine two instances of p, representing an upper limit p_{up} and a lower limit p_{low} (upper and lower edge of gray boxes in figure D1(a)). The upper limit p_{up} is obtained by solving equation (D.3) for the median of the extinction probabilities Ω of all species with a degree $k = 1$ in the exemplary network, while p_{low} is set to the median of the extinction probabilities Ω of all species with a degree $k > 7$, as $p^k \to 0$ for $p \ll 1$ and $k \gg 1$.

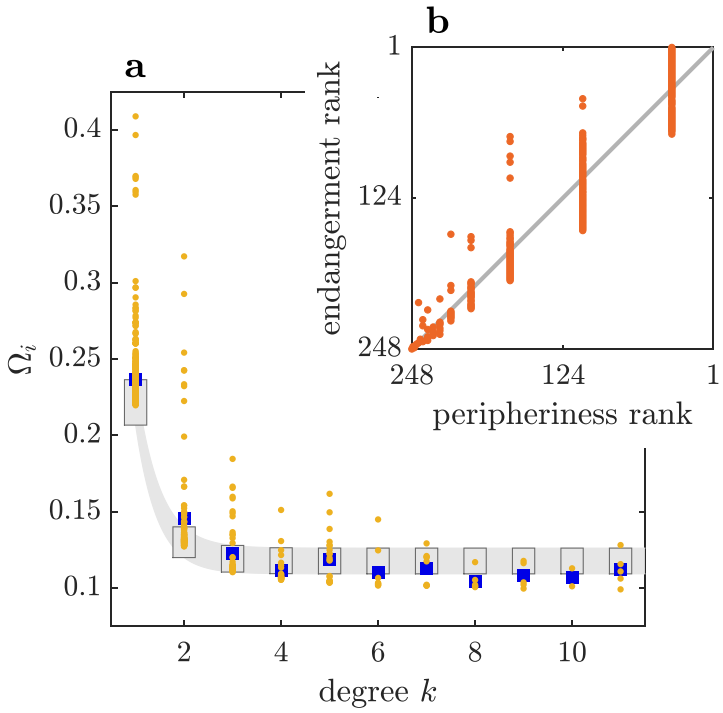

Figure D1. Comparison between the endangerment in the complete and the strongly simplified model. (a) Dependence of the extinction probability Ω_i on the degree. Yellow dots correspond to Ω_i of species in the dynamic model of the exemplary mutualistic system (M_PL_044 in table A1). Blue squares represent the median of Ω for all species with the same degree. Gray boxes correspond to the Ω_i provided by the simplified model (equation (D.3)), where the upper edge is determined by adaptation to the specialists ($k = 1$) and the lower bound by adaptation to the generalists ($k > 7$). (b) Rank correlation between peripheriness (inverse centrality) measured by degree and endangerment measured by Ω.

The comparison shows that the endangerment distribution obtained from the complete dynamical model generally follows the dependency described by equation (D.3) (figure D1(a)). Accordingly, the degree is an important driver of a species' endangerment. However, we observe that species with the same degree strongly differ in their endangerment and that the simple approximation is not able to capture the exceptional endangerment of some species (especially in the specialist class). Accordingly, the degree is an important but not the only driver of a species' endangerment.

We furthermore find that, if adapted to the endangerment of generalists (p_{low}), the simplified model underestimates the endangerment of specialists. This indicates that the simplification might not capture all aspects which cause the particular endangerment of specialists—for instance, the simplified model does not take into account that shock perturbations affect the mutualistic term m_i (equation (4), but see appendix E).

Appendix E. Mutualistic benefit after a shock

The relation between the degree of specialization and the endangerment of a species, as derived in appendix D, was based on the assumption that mutualistic benefits were fully present (saturated) as long as any partner species was left. This does of course neglect an integral element of the mutualistic system, which is the term describing the actual mutualistic benefit m_i a species obtains from the interaction with its partners (equation (4)).

The mutualistic benefit m_i depends on the number and abundance of partner species. Accordingly, since the abundances of species constitute the state variables of the system, the mutualistic benefit is a dynamic, time-dependent quantity, $m_i(\mathbf{A}(t))$. However, for the sake of simplicity, we consider m_i at one particular point in time, $t = 0$, which is the time at which the shock perturbation has just hit the system. In other words, we simply examine how the perturbation shapes the mutualistic benefit m_i. At $t = 0$, the abundance of each species can be considered as a random variable drawn from a uniform distribution in the interval $[0, N_j^*]$, where N_j^* is the abundance of species j in the desired or pre-disturbance state (see section 2.2). Assuming for now that N_j^* is the same for all species ($N_j^* = N^*$), we can derive a probability distribution for the mutualistic

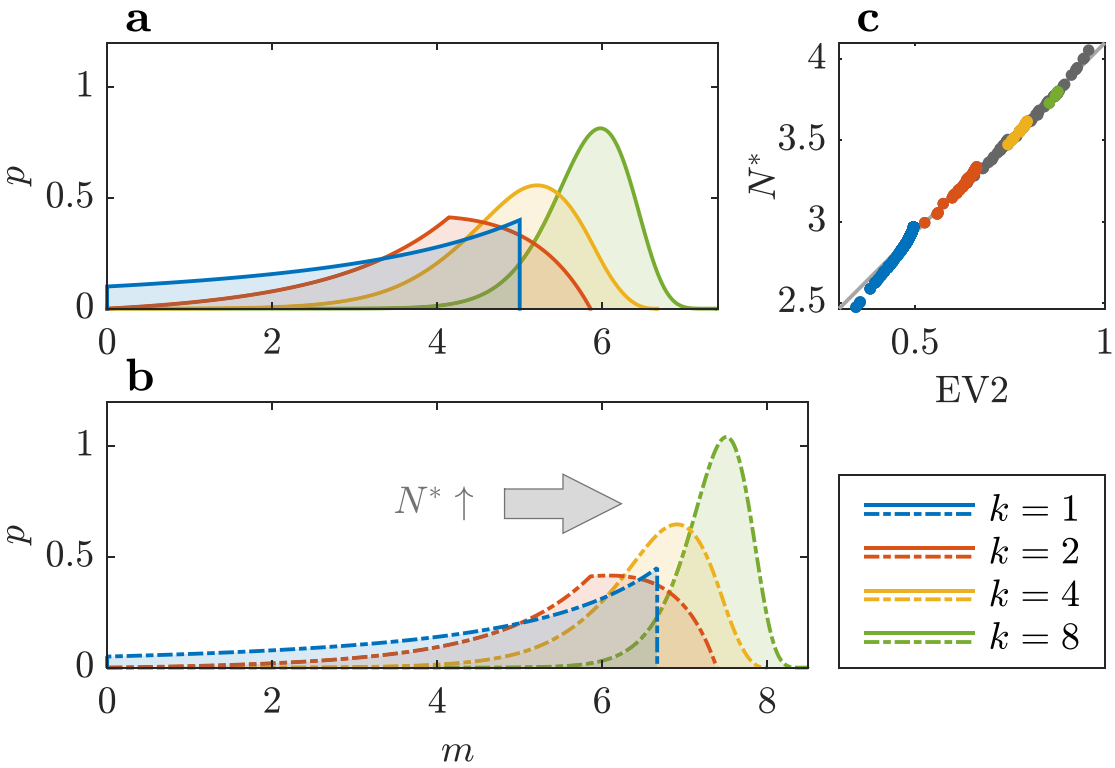

Figure E1. Probabilistic description of the mutualistic term m_i at $t = 0$. (a) and (b) probability distribution of the mutualistic benefit for different degrees k for $N^* = 1.0$ (a) and $N^* = 2.0$ (b). (c) Correlation between the EV2 and the abundance of species N^* in the desired state in the exemplary mutualistic system (M_PL_044 in table A1).

benefit m_i using a transformation of the Irwin–Hall distribution [96]. The resulting probability density function is

$$f_y = \frac{1}{(k-1)!} \sum_{j=0}^{\left\lfloor \frac{y}{\gamma N^* (1-hy)} \right\rfloor} (-1)^j \binom{k}{j} \frac{1}{\gamma N^* (1-hy)^2} \cdot \left(\frac{y}{\gamma N^* - \gamma N^* hy} - j \right)^{k-1}, \tag{E.1}$$

with $\gamma = \gamma_i = \gamma_0 / k_i^{\zeta}$ and $\lfloor \cdot \rfloor$ being the floor function.

Admittedly, equation (E.1) is a little difficult to read. Therefore, to understand the impact of the degree k and the abundance of partners N^* on the mutualistic benefit m_i which remains after a perturbation, the inspection of exemplary probability distributions for specific k and N^* is instructive (figures E1(a) and (b)). Regarding the impact of the remaining mutualistic benefit on the endangerment of a species, it can be assumed that very low $m_i(t = 0)$ are particularly dangerous since they can cause an overall negative growth rate (equation (1)) at the time of the shock perturbation ($t = 0$).

Regarding the impact of the degree k, we note that the degree affects both the position and the shape of the probability distribution of the mutualistic benefit $m_i(t = 0)$ (figure E1(a)). Due to the specific shape of the distribution for low degrees, especially for $k = 1$, very low $m_i(t = 0)$ are way more probable for specialists than for less specialized species ($k > 1$). The way in which the mutualistic benefit m_i is affected by the shock perturbation thus reveals another aspect amplifying the particular endangerment of specialists.

In contrast to the degree, the abundance of partners N^* mainly affects the position of the probability distribution of $m_i(t = 0)$—an increase of N^* leads to a distortion of the probability distribution towards larger mutualistic benefits m_i, while the specific shape of the curve is basically maintained (see change from figures E1(a) and (b)). This means that the chance of receiving a very low m_i right after a perturbation decreases significantly for species whose partners have a high abundance in the undisturbed system state. However, the abundance N^* is not the same for all species but relies on the species' position within the network. In fact, we find a strong correlation between the abundance N_i^* and the centrality of the corresponding node, a relation which is well captured by the EV2 (figure E1(c)). Accordingly, species whose partners show a low EV2 score—corresponding to peripheral nodes—have a higher chance of receiving a low mutualistic benefit after the shock perturbation than species which are linked to species in the core of the network (high EV2).

References

[1] Boucher D H, James S and Keeler K H 1982 The ecology of mutualism *Ann. Rev. Ecol. Syst.* **13** 315–47
[2] Bronstein J L 2015 *Mutualism* (Oxford University Press)
[3] Jordano P, Bascompte J and Olesen J M 2003 Invariant properties in coevolutionary networks of plant–animal interactions *Ecol. Lett.* **6** 69–81
[4] Bascompte J, Jordano P, Melián C J and Olesen J M 2003 The nested assembly of plant–animal mutualistic networks *Proc. Natl Acad. Sci.* **100** 9383–7
[5] Memmott J, Waser N M and Price M V 2004 Tolerance of pollination networks to species extinctions *Proc. R. Soc. B* **271** 2605–11
[6] Bastolla U, Fortuna M A, Pascual-García A, Ferrera A, Luque B and Bascompte J 2009 The architecture of mutualistic networks minimizes competition and increases biodiversity *Nature* **458** 1018–20
[7] Thébault E and Fontaine C 2010 Stability of ecological communities and the architecture of mutualistic and trophic networks *Science* **329** 853–6
[8] Bascompte J and Jordano P 2013 *Mutualistic Networks* vol 70 (Princeton University Press)
[9] Suweis S, Simini F, Banavar J R and Maritan A 2013 Emergence of structural and dynamical properties of ecological mutualistic networks *Nature* **500** 449–52
[10] Rohr R P, Saavedra S and Bascompte J 2014 On the structural stability of mutualistic systems *Science* **345** 1253497
[11] Kaiser-Bunbury C N, Muff S, Memmott J, Müller C B and Caflisch A 2010 The robustness of pollination networks to the loss of species and interactions: a quantitative approach incorporating pollinator behaviour *Ecol. Lett.* **13** 442–52
[12] Vieira M C, Almeida-Neto M and Irwin R 2015 A simple stochastic model for complex coextinctions in mutualistic networks: robustness decreases with connectance *Ecol. Lett.* **18** 144–52
[13] Domínguez-García V and Munoz M A 2015 Ranking species in mutualistic networks *Sci. Rep.* **5** 8182
[14] Potts S G, Biesmeijer J C, Kremen C, Neumann P, Schweiger O and Kunin W E 2010 Global pollinator declines: trends, impacts and drivers *Trends Ecol. Evol.* **25** 345–53
[15] Burkle L A, Marlin J C and Knight T M 2013 Plant-pollinator interactions over 120 years: loss of species, co-occurrence and function *Science* **339** 1611–5
[16] Saavedra S, Stouffer D B, Uzzi B and Bascompte J 2011 Strong contributors to network persistence are the most vulnerable to extinction *Nature* **478** 233–5
[17] James A, Pitchford J W and Plank M J 2012 Disentangling nestedness from models of ecological complexity *Nature* **487** 227–30
[18] Vázquez D P and Aizen M A 2004 Asymmetric specialization: a pervasive feature of plant–pollinator interactions *Ecology* **85** 1251–7
[19] Csermely P, London A, Ling-Yun W and Uzzi B 2013 Structure and dynamics of core/periphery networks *J. Complex Netw.* **1** 93–123
[20] Lee S H *et al* 2016 Network nestedness as generalized core-periphery structures *Phys. Rev. E* **93** 022306
[21] Miele V, Ramos-Jiliberto R, Vázquez D P and Rodriguez-Cabal M 2020 Core–periphery dynamics in a plant–pollinator network *J. Animal Ecol.* **89** 1670–7
[22] Seidman S B 1983 Network structure and minimum degree *Soc. Netw.* **5** 269–87
[23] Morone F, Ferraro G D and Makse H A 2019 The k-core as a predictor of structural collapse in mutualistic ecosystems *Nat. Phys.* **15** 95–102
[24] Saavedra S, Rohr R P, Dakos V and Bascompte J 2013 Estimating the tolerance of species to the effects of global environmental change *Nat. Commun.* **4** 2350
[25] Lever J J, van Nes E H, Scheffer M, Bascompte J and Jordan F 2014 The sudden collapse of pollinator communities *Ecol. Lett.* **17** 350–9
[26] Dakos V and Bascompte J 2014 Critical slowing down as early warning for the onset of collapse in mutualistic communities *Proc. Natl Acad. Sci.* **111** 17546–51
[27] Jiang J, Huang Z-G, Seager T P, Lin W, Grebogi C, Hastings A and Lai Y-C 2018 Predicting tipping points in mutualistic networks through dimension reduction *Proc. Natl Acad. Sci.* **115** E639–47
[28] Lever J J, van de Leemput I A, Weinans E, Quax R, Dakos V, van Nes E H, Bascompte J, Scheffer M and Drake J 2020 Foreseeing the future of mutualistic communities beyond collapse *Ecol. Lett.* **23** 2–15
[29] Aparicio A, Velasco-Hernández J X, Moog C H, Liu Y-Y and Angulo M T 2021 Structure-based identification of sensor species for anticipating critical transitions *Proc. Natl Acad. Sci.* **118** e2104732118
[30] Wu C and Duan D 2024 Collapse process prediction of mutualistic dynamical networks with k-core and dimension reduction method *Chaos Solitons Fractals* **180** 114489
[31] Chattopadhyay A, Samadder A, Mukhopadhyay S, Bhattacharya S and Lai Y-C 2025 Understanding pesticide-induced tipping in plant-pollinator networks across geographical scales: Prioritizing richness and modularity over nestedness *Phys. Rev. E* **111** 014407
[32] Bascompte J and Scheffer M 2023 The resilience of plant–pollinator networks *Ann. Rev. Entomol.* **68** 363–80
[33] Latty T and Dakos V 2019 The risk of threshold responses, tipping points and cascading failures in pollination systems *Biodiver. Conserv.* **28** 1–18
[34] Baruah G 2023 Transitions and its indicators in mutualistic meta-networks: effects of network topology, size of metacommunities and species dispersal *Evol. Ecol.* **37** 691–708
[35] Scheffer M, Carpenter S, Foley J A, Folke C and Walker B 2001 Catastrophic shifts in ecosystems *Nature* **413** 591–6
[36] Coumou D and Rahmstorf S 2012 A decade of weather extremes *Nat. Clim. Change* **2** 491–6
[37] Goulson D, Nicholls E, Botías C and Rotheray E L 2015 Bee declines driven by combined stress from parasites, pesticides and lack of flowers *Science* **347** 1255957
[38] Soroye P, Newbold T and Kerr J 2020 Climate change contributes to widespread declines among bumble bees across continents *Science* **367** 685–8
[39] Harvey J A, Heinen R, Gols R and Thakur M P 2020 Climate change-mediated temperature extremes and insects: from outbreaks to breakdowns *Glob. Change Biol.* **26** 6685–701
[40] Halsch C A, Shapiro A M, Fordyce J A, Nice C C, Thorne J H, Waetjen D P and Forister M L 2021 Insects and recent climate change *Proc. Natl Acad. Sci.* **118** 3117
[41] Wagner D L, Fox R, Salcido D M and Dyer L A 2021 A window to the world of global insect declines: moth biodiversity trends are complex and heterogeneous *Proc. Natl Acad. Sci.* **118** 49117
[42] Feng W and Bailey R M 2018 Unifying relationships between complexity and stability in mutualistic ecological communities *J. Theor. Biol.* **439** 100–26

[43] Scheffer M, Bascompte J, Brock W A, Brovkin V, Carpenter S R, Dakos V, Held H, Van Nes E H, Rietkerk M and Sugihara G 2009 Early-warning signals for critical transitions *Nature* **461** 53–59
[44] Halekotte L and Feudel U 2020 Minimal fatal shocks in multistable complex networks *Sci. Rep.* **10** 1–13
[45] Nitzbon J, Schultz P, Heitzig J, Kurths J and Hellmann F 2017 Deciphering the imprint of topology on nonlinear dynamical network stability *New J. Phys.* **19** 033029
[46] Zhang H, Wang Q, Zhang W, Havlin S and Gao J 2022 Estimating comparable distances to tipping points across mutualistic systems by scaled recovery rates *Nat. Ecol. Evol.* **6** 1524–36
[47] Xu F, Jin M, Shen C, Qi H, Huang S, Wang M, Zhang J and Li X 2025 Biodiversity-induced opposing shifts of tipping points in mutualistic ecological networks *Chaos* **35** 053138
[48] Courchamp F, Berec L and Gascoigne J 2008 *Allee Effects in Ecology and Conservation* (Oxford University Press)
[49] Darvill B, Ellis J S, Lye G C and Goulson D 2006 Population structure and inbreeding in a rare and declining bumblebee, bombus muscorum (hymenoptera: Apidae) *Mol. Ecol.* **15** 601–11
[50] Berec L, Angulo E and Courchamp F 2007 Multiple Allee effects and population management *Trends Ecol. Evol.* **22** 185–91
[51] Busch J W and Schoen D J 2008 The evolution of self-incompatibility when mates are limiting *Trends Plant Sci.* **13** 128–36
[52] Ansmann G 2018 Efficiently and easily integrating differential equations with JiTCODE, JiTCDDE, and JiTCSDE *Chaos* **28** 043116
[53] Lü L, Chen D, Ren X-L, Zhang Q-M, Zhang Y-C and Zhou T 2016 Vital nodes identification in complex networks *Phys. Rep.* **650** 1–63
[54] Liao H, Mariani M S, Medo M, Zhang Y-C and Zhou M-Y 2017 Ranking in evolving complex networks *Phys. Rep.* **689** 1–54
[55] Bonacich P 1987 Power and centrality: a family of measures *Am. J. Sociol.* **92** 1170–82
[56] Kitsak M, Gallos L K, Havlin S, Liljeros F, Muchnik L, Eugene Stanley H and Makse H A 2010 Identification of influential spreaders in complex networks *Nat. Phys.* **6** 888–93
[57] Zeng A and Zhang C-J 2013 Ranking spreaders by decomposing complex networks *Phys. Lett. A* **377** 1031–5
[58] Bae J and Kim S 2014 Identifying and ranking influential spreaders in complex networks by neighborhood coreness *Physica A* **395** 549–59
[59] Liu J-G, Lin J-H, Guo Q and Zhou T 2016 Locating influential nodes via dynamics-sensitive centrality *Sci. Rep.* **6** 21380
[60] Ma L-L, Ma C, Zhang H-F and Wang B-H 2016 Identifying influential spreaders in complex networks based on gravity formula *Physica A* **451** 205–12
[61] Liu Y, Tang M, Zhou T and Do Y 2016 Identify influential spreaders in complex networks, the role of neighborhood *Physica A* **452** 289–98
[62] Kato M 2000 Anthophilous insect community and plant-pollinator interactions on Amami Islands in the Ryukyu Archipelago, Japan *Contr. Biol. Lab. Kyoto Univ.* **29** 157–254
[63] Kamada T *et al* 1989 An algorithm for drawing general undirected graphs *Inf. Process. Lett.* **31** 7–15
[64] Kendall M G 1938 A new measure of rank correlation *Biometrika* **30** 81–93
[65] Ahajjam S and Badir H 2018 Identification of influential spreaders in complex networks using hybridrank algorithm *Sci. Rep.* **8** 1–10
[66] Erkol Şirag, Castellano C and Radicchi F 2019 Systematic comparison between methods for the detection of influential spreaders in complex networks *Sci. Rep.* **9** 15095
[67] Gracia-Lázaro C, Hernández L, Borge-Holthoefer J and Moreno Y 2018 The joint influence of competition and mutualism on the biodiversity of mutualistic ecosystems *Sci. Rep.* **8** 1–9
[68] Vanselow A, Halekotte L and Feudel U 2022 Evolutionary rescue can prevent rate-induced tipping *Theor. Ecol.* **15** 29–50
[69] Newman M 2018 *Networks* (Oxford University Press)
[70] Aizen M A, Sabatino M and Tylianakis J M 2012 Specialization and rarity predict nonrandom loss of interactions from mutualist networks *Science* **335** 1486–9
[71] Morton D N, Keyes A, Barner A K and Dee L E 2022 Merging theory and experiments to predict and understand coextinctions *Trends Ecol. Evol.* **37** 886–98
[72] Fortuna M A and Bascompte J 2006 Habitat loss and the structure of plant–animal mutualistic networks *Ecol. Lett.* **9** 281–6
[73] Ren P, Didham R K, Murphy M V, Zeng Di, Si X and Ding P 2023 Forest edges increase pollinator network robustness to extinction with declining area *Nat. Ecol. Evol.* **7** 393–404
[74] Vanbergen A J, Woodcock B A, Heard M S, Chapman D S and Brody A 2017 Network size, structure and mutualism dependence affect the propensity for plant–pollinator extinction cascades *Funct. Ecol.* **31** 1285–93
[75] Blüthgen N 2010 Why network analysis is often disconnected from community ecology: a critique and an ecologist's guide *Basic Appl. Ecol.* **11** 185–95
[76] Bertness M D and Callaway R 1994 Positive interactions in communities *Trends Ecol. Evol.* **9** 191–3
[77] He Q, Bertness M D, Altieri A H and Vila M 2013 Global shifts towards positive species interactions with increasing environmental stress *Ecol. Lett.* **16** 695–706
[78] Pianosi F, Beven K, Freer J, Hall J W, Rougier J, Stephenson D B and Wagener T 2016 Sensitivity analysis of environmental models: a systematic review with practical workflow *Environ. Modelling Softw.* **79** 214–32
[79] Westrich P 2018 *Die Wildbienen Deutschlands* (Verlag Eugen Ulmer)
[80] Halekotte L, Vanselow A and Feudel U 2021 Transient chaos enforces uncertainty in the British power grid *J. Phys. Complex.* **2** 035015
[81] Krönke J, Wunderling N, Winkelmann R, Staal A, Stumpf B, Tuinenburg O A and Donges J F 2020 Dynamics of tipping cascades on complex networks *Phys. Rev. E* **101** 042311
[82] Meyer K, Hoyer-Leitzel A, Iams S, Klasky I, Lee V, Ligtenberg S, Bussmann E and Zeeman M L 2018 Quantifying resilience to recurrent ecosystem disturbances using flow–kick dynamics *Nat. Sustain.* **1** 671–8
[83] Vanselow A, Wieczorek S and Feudel U 2019 When very slow is too fast-collapse of a predator-prey system *J. Theor. Biol.* **479** 64–72
[84] Harris R M B *et al* 2018 Biological responses to the press and pulse of climate trends and extreme events *Nat. Clim. Change* **8** 579–87
[85] Suweis S, Grilli J, Banavar J R, Allesina S and Maritan A 2015 Effect of localization on the stability of mutualistic ecological networks *Nat. Commun.* **6** 10179
[86] Clements F E and Long F L 1923 *Experimental Pollination: an Outline of the Ecology of Flowers and Insects* (Carnegie institution of Washington)
[87] Petanidou T 1991 Pollination ecology in a phryganic ecosystem *PhD Thesis* Aristotelian University, Thessaloniki, Greece
[88] Kato M, Kakutani T, Inoue T and Itino T 1990 Insect-flower relationship in the primary beech forest of Ashu, Kyoto: an overview of the flowering phenology and the seasonal pattern of insect visits *Contr. Biol. Lab. Kyoto Univ.* **27** 309–76

[89] Dupont Y L and Olesen J M 2009 Ecological modules and roles of species in heathland plant-insect flower visitor networks *J. Animal Ecol.* **78** 346–53
[90] Bek S 2006 A pollination network from a Danish forest meadow *MSc Thesis* Aarhus University, Aarhus, Denmark
[91] Yamazaki K and Kato M 2003 Flowering phenology and anthophilous insect community in a grassland ecosystem at Mt. Yufu, Western Japan *Contr. Biol. Lab. Kyoto Univ.* **29** 255
[92] Kakutani T, Inoue T, Kato M and Ichihashi H 1990 Insect-flower relationship in the campus of Kyoto University, Kyoto: an overview of the flowering phenology and the seasonal pattern of insect visits *Contr. Biol. Lab. Kyoto Univ.* **27** 465–522
[93] Kato M and Miura R 1996 Flowering phenology and anthophilous insect community at a threatened natural lowland marsh at Nakaikemi in Tsuruga, Japan *Contr. Biol. Lab. Kyoto Univ.* **29** 1
[94] Kato M, Matsumoto M and Kato Tôru 1993 Flowering phenology and anthophilous insect community in the cool-temperate subalpine forests and meadows at Mt. Kushigata in the central part of Japan *Contr. Biol. Lab. Kyoto Univ.* **28** 119–72
[95] Inoue T, Kato M, Kakutani T, Suka T and Itino T 1990 Insect-flower relationship in the temperate deciduous forest of Kibune, Kyoto: an overview of the flowering phenology and the seasonal pattern of insect visits *Contr. Biol. Lab. Kyoto Univ.* **27** 377–464
[96] Johnson N L, Kotz S and Balakrishnan N 1995 *Continuous Univariate Distributions* vol 2 (Wiley) p 289